High Energy Physics Revista Mexicana de Física **72** 050801 1–14 SEPTEMBER-OCTOBER 2026

Systematic analysis of fermionic masses and flavor mixings: a model-independent approach

E. Barradas-Guevara[a], O. Félix-Beltrán[b], F. González-Canales[b], V. Luna-Mendoza[a], A. Pérez-Martínez[b], and M. Ramos-Martínez[a]

[a]*Facultad de Ciencias Físico Matemáticas, Benemérita Universidad Autónoma de Puebla, Apartado Postal 1152, Puebla, 72000, Pue., México.*
[b]*Facultad de Ciencias de la Electrónica, Benemérita Universidad Autónoma de Puebla, Apartado Postal 542, Puebla, 72570, Pue., México.*

Received 17 July 2025; accepted 16 April 2026

In a model-independent context, we perform a systematic and detailed study of the fermion flavor masses and mixings. In this analysis, we present a most general parameterization form of the 3×3 mass matrix, as well as the Pontecorvo-Maki-Nakagawa-Sakata flavor mixing matrix, in terms of the fermionic masses and some free parameters. A likelihood test using the χ^2 statistic is implemented to evaluate whether the theoretical expressions for the leptonic flavor mixing angles also reproduce the experimental data. The results of the χ^2 fit show that the theoretical expressions obtained for the Pontecorvo-Maki-Nakagawa-Sakata mixing matrix correctly reproduce the actual experimental data on neutrino oscillations.

Keywords: Fermionic mass matrix; fermionic mixing matrix.

DOI: https://doi.org/10.31349/RevMexFis.72.050801

1. Introduction

The fermionic sector of particle physics deserves an in-depth exploration beyond the Standard Model for several fundamental reasons. The Standard Model, although successful, has critical gaps in that sector [1-4], as it does not explain why exactly three generations of fermions exist, nor does it predict their specific masses [1,5]. The hierarchy of fermionic masses, from the neutrino to the top quark, spans more than 12 orders of magnitude without a satisfactory theoretical explanation. The mixing patterns in the fermionic sector reveal structures that suggest deeper underlying physics. The CKM matrix for quarks and the PMNS matrix for neutrinos show mixing angles that appear to follow specific patterns, but the Standard Model offers no fundamental explanation for these values. In concordance with experiments [6,7], neutrinos oscillation is given by impliying the massive neutrinos [1]. On the other hand, the CP violation observed in the fermionic sector is insufficient to explain the matter-antimatter asymmetry of the universe. This suggests that additional sources of CP violation exist in extended fermionic sectors. Many dark matter candidates are fermionic (such as neutralinos in supersymmetry). Exploration of the extended fermionic sector could reveal stable particles that constitute dark matter. Standard Model fermions naturally fit into representations of larger symmetry groups (such as SO(10) or E6), suggesting that they are part of more fundamental structures. Exploration of the fermionic sector transcends current limitations and could reveal the fundamental architecture of physical reality, connecting from microscopic structure to the deepest cosmological mysteries.

Within the SM framework, neutrinos were originally considered massless particles, since they do not interact with the Higgs field in the same way as other particles. However, in SM minimal extensions, such as the See-Saw mechanism, a natural explanation is introduced for the extremely small neutrino masses. In this model, neutrinos acquire mass through mixing with heavier particles, which results in neutrino masses being much smaller compared to other particles [8]. Although the absolute neutrino mass has not yet been directly measured, very low upper limits ($O(\mathrm{eV})$) have been set by experiments such as KATRIN [9]. These experiments confirm that neutrinos have an extremely small, but nonzero, mass.

This paper is organized as follow: Section 2 is addressed to the fermionic mixing matrices, whereas Sec. 3 shows the fermionic general mass matrix and its analysis; the orthogonal matrix associated to the diagonalization of the general mass matrix is shown in Sec. 4. The analytic lepton flavor mixing matrix and numerical analysis is provided in Sec. 5. Finally, in Sec. 6 are given the conclusions.

2. Fermionic Mixing matrices

CKM matrix

The CKM matrix $\mathbf{V}_{\mathrm{CKM}}$ (Cabibbo, Kobayashi, Maskawa) is of the order 3×3 that describes quark mixings in SM context. This one specifically refers how up (u, c, t)-down (d, s, b) quarks mix through the weak interaction. This mixing is related with disintegration processes mediated for $W^{\pm}$ gauge bosons (charged currents) and quarks flavor changing. The $\mathbf{V}_{\mathrm{CKM}}$ has the form [1]:

$$\mathbf{V}_{\text{CKM}} = \mathbf{U}_u \mathbf{U}_d^\dagger = \begin{pmatrix} V_{ud} & V_{us} & V_{ub} \\ V_{cd} & V_{cs} & V_{cb} \\ V_{td} & V_{ts} & V_{tb} \end{pmatrix}, \quad (1)$$

where $\mathbf{U}_u$ and $\mathbf{U}_d$ are unitary matrices that diagonalize the mass matrix of the up- and down-quarks, respectively. The elements of the CKM matrix $[\mathbf{V}_{\text{CKM}}]_{ij}$ are complex numbers that describe the transition probability from a quark i-th to a quark j-th. Since the CKM matrix $\mathbf{V}_{\text{CKM}}$ is unitary, guarantees the conservation of probability in transitions between quarks. In an angle-phase parameterization, the matrix elements are related to three mixing angles (θ_{12}, θ_{23}, θ_{13}), and one Charge-Parity (CP)- violating phase, δ_{CP}. These mixing angles determine the magnitude of mixing between quarks, while the phase is responsible for CP symmetry violation in weak interactions. The complex phase of the $\mathbf{V}_{\text{CKM}}$ is the source that introduces CP violation in the SM, a phenomenon related to the fact that the laws of physics are not completely symmetric under charge and parity inversion.

In the standard PDG parameterization, the $\mathbf{V}_{\text{CKM}}$ is written as [1]

$$\mathbf{V}_{\text{CKM}} = \begin{pmatrix} c_{12}c_{13} & s_{12}c_{13} & s_{13}e^{-i\delta} \\ -s_{12}c_{23} - c_{12}s_{23}s_{13}e^{i\delta} & c_{12}c_{23} - s_{12}s_{23}s_{13}e^{i\delta} & s_{23}c_{13} \\ s_{12}s_{23} - c_{12}c_{23}s_{13}e^{i\delta} & -c_{12}s_{23} - s_{12}c_{23}s_{13}e^{i\delta} & c_{23}c_{13} \end{pmatrix}, \quad (2)$$

where $s_{ij} \equiv \sin\theta_{ij}$ and $c_{ij} \equiv \cos\theta_{ij}$. The meaning of the mixing angles are: θ_{12} represents the mixing between the first and second generation of quarks, whereas θ_{23} angle represents the mixing between the second and third generation of quarks, and θ_{13} angle represents the mixing between the first and third generation of quarks. This angle is associated with the complex phase δ_{CP}, which is crucial for CP violation. The elements of the CKM matrix are related to three mixing angles in the following form [10],

$$\sin^2\theta_{12} = \frac{|V_{us}|^2}{1-|V_{ub}|^2},$$
$$\sin^2\theta_{23} = \frac{|V_{cb}|^2}{1-|V_{ub}|^2},$$
$$\sin^2\theta_{13} = |V_{ub}|^2. \quad (3)$$

On the other hand, the Jarlskog invariant is a scalar quantity that measures the magnitude of CP symmetry violation in the quark sector of the Standard Model. It is defined from the elements of the CKM matrix; specifically, the Jarlskog invariant is expressed as [11]:

$$\mathcal{J} = \mathbb{I}m\left\{V_{ud}V_{cs}V_{us}^*V_{cd}^*\right\}. \quad (4)$$

This invariant is particularly important because it does not depend on the choice of the phase in the CKM matrix. Its value is proportional to the magnitude of CP symmetry violation in quark interactions, serving as a direct indicator of this phenomenon. In terms of the mixing angles, we have

$$\mathcal{J} = \frac{1}{8}\sin 2\theta_{12}\sin 2\theta_{23}\sin 2\theta_{13}\cos\theta_{13}\sin\delta_{CP}. \quad (5)$$

Thus, the phase factor in terms of the elements of the $\mathbf{V}_{\text{CKM}}$ can be written as:

$$\sin\delta_{CP} = \frac{\mathcal{J}\left(1-|V_{ub}|^2\right)}{|V_{cb}||V_{tb}||V_{ub}||V_{ud}||V_{us}|}. \quad (6)$$

To arrive at the above expression, the fact that the $\mathbf{V}_{\text{CKM}}$ is unitary was used.

PMNS matrix

The PMNS matrix (Pontecorvo-Maki-Nakagawa-Sakata) is analogous to the CKM matrix but applies to the lepton sector instead of the quark sector (it is crucial for describing how neutrinos change from one type to another, a phenomenon known as neutrino oscillation). The PMNS matrix relates the flavor states of leptons to their mass states. The leptonic flavor mixing matrix PMNS arises from the mismatch between the diagonalization of the charged lepton and neutrino mass matrices, and is defined as [1],

$$\mathbf{V}_{\text{PMNS}} = \mathbf{U}_\ell^\dagger \mathbf{U}_\nu = \begin{pmatrix} U_{e1} & U_{e2} & U_{e3} \\ U_{\mu 1} & U_{\mu 2} & U_{\mu 3} \\ U_{\tau 1} & U_{\tau 2} & U_{\tau 3} \end{pmatrix}, \quad (7)$$

where $\mathbf{U}_\ell$ and $\mathbf{U}_\nu$ are unitary matrices that diagonalize the mass matrices of the charged leptons and neutrinos, respectively. Each element $U_{\alpha i}$ of the PMNS matrix describes the probability amplitude for a neutrino with flavor α (where α can be e, μ, or τ) to be in the mass state i (where $i = 1, 2$, or 3). In the symmetric parametrization of the PMNS matrix, three mixing angles (θ_{12}, θ_{23}, θ_{13}) and three CP-violating phases $(\phi_{12}, \phi_{13}, \phi_{23})$ are included [12]. In this parametrization, the PMNS matrix is written as [1]

$$\mathbf{V}_{\text{PMNS}} = \begin{pmatrix} c_{12}c_{13} & s_{12}c_{13}e^{-i\phi_{12}} & s_{13}e^{-i\phi_{13}} \\ -s_{12}c_{23}e^{i\phi_{12}} - c_{12}s_{23}s_{13}e^{-i(\phi_{23}-\phi_{13})} & c_{12}c_{23} - s_{12}s_{23}s_{13}e^{-i(\phi_{23}+\phi_{12}-\phi_{13})} & s_{23}c_{13}e^{-i\phi_{23}} \\ s_{12}s_{23}e^{i(\phi_{23}+\phi_{12})} - c_{12}c_{23}s_{13}e^{i\phi_{13}} & -c_{12}s_{23}e^{i\phi_{23}} - s_{12}c_{23}s_{13}e^{-i(\phi_{12}-\phi_{13})} & c_{23}c_{13} \end{pmatrix}, \quad (8)$$

where $s_{ij} = \sin\theta_{ij}$ and $c_{ij} = \cos\theta_{ij}$. The relations between the mixing angles and the entries of the PMNS matrix are

$$\sin^2\theta_{12} = \frac{|U_{e2}|^2}{1 - |U_{e3}|^2},$$
$$\sin^2\theta_{23} = \frac{|U_{\mu 3}|^2}{1 - |U_{e3}|^2},$$
$$\sin^2\theta_{13} = |U_{e3}|^2. \tag{9}$$

In case of neutrino oscillations, the Jarlskog invariant is defined as

$$\mathcal{J} = \mathbb{I}m\left\{U_{e1}U_{\mu 3}U_{e3}^{*}U_{\mu 1}^{*}\right\}, \tag{10}$$

which in the symmetric parametrization takes the form

$$\mathcal{J} = \frac{1}{8}\sin 2\theta_{12}\sin 2\theta_{23}\sin 2\theta_{13}\cos\theta_{13}\sin\delta, \tag{11}$$

where $\delta = \phi_{13} - \phi_{23} - \phi_{12}$. In addition, the invariants

$$\mathcal{I}_1 = \mathbb{I}m\left\{U_{e2}^2 U_{e1}^{*2}\right\},$$
$$\mathcal{I}_2 = \mathbb{I}m\left\{U_{e3}^2 U_{e1}^{*2}\right\}, \tag{12}$$

associated with the Majorana phase factors [10] in the symmetric parametrization take the form

$$\mathcal{I}_1 = \frac{1}{4}\sin^2 2\theta_{12}\cos^4\theta_{13}\sin\left(-2\phi_{12}\right),$$
$$\mathcal{I}_2 = \frac{1}{4}\sin^2 2\theta_{13}\cos^2\theta_{12}\sin\left(-2\phi_{13}\right). \tag{13}$$

Then, the phase factors associated with CP violation can be written as

$$\sin\delta = \frac{\mathcal{J}\left(1 - |V_{e3}|^2\right)}{|U_{e1}|\,|U_{e2}|\,|U_{e3}|\,|U_{\mu 3}|\,|U_{\tau 3}|},$$
$$\sin\left(-2\phi_{12}\right) = \frac{\mathcal{I}_1}{|U_{e1}|^2\,|U_{e2}|^2},$$
$$\sin\left(-2\phi_{13}\right) = \frac{\mathcal{I}_1}{|U_{e1}|^2\,|U_{e3}|^2}. \tag{14}$$

The equivalence between the standard PDG parametrization and the symmetric one can be expressed as $\mathbf{U}_{\text{PDG}} = \mathbf{K}\mathbf{U}_{\text{sim}}$, where $\mathbf{K} = \text{diag}\left(1, e^{i(\alpha_{21}/2)}, e^{i(\alpha_{21}/2)}\right)$. Here, the Dirac-type phase takes the form $\delta = \phi_{13} - \phi_{23} - \phi_{12}$, while the Majorana-type phases are $\alpha_{21} = -2\phi_{12}$ and $\alpha_{31} = -2\left(\phi_{12} + \phi_{23}\right)$.

3. Fermionic general mass matrix

In general, in the physics of elementary particles, the fermionic mass matrix, $\mathbf{M}_f$, does not have any particular internal symmetry. Therefore, to diagonalize it through a unitary transformation, bilinear forms must be constructed as follows:

$$\mathbf{M}_f\mathbf{M}_f^{\dagger} \quad \text{and} \quad \mathbf{M}_f^{\dagger}\mathbf{M}_f, \tag{15}$$

which are Hermitian matrices. The matrices in Eq. (15) can be brought to their diagonal form through the following unitary transformations:

$$\mathbf{V}_f\mathbf{M}_f\mathbf{M}_f^{\dagger}\mathbf{V}_f^{\dagger} = \mathbf{\Delta}_{f,\lambda} \quad \text{and}$$
$$\mathbf{U}_f\mathbf{M}_f^{\dagger}\mathbf{M}_f\mathbf{U}_f^{\dagger} = \mathbf{\Delta}_{f,\lambda}, \tag{16}$$

where $\mathbf{U}_f$ and $\mathbf{V}_f$ are unitary matrices. Additionally, $\mathbf{\Delta}_{f,\lambda} = \text{diag}\left(\lambda_{f1}, \lambda_{f2}, \lambda_{f3}\right)$, where the λ_{fi} are the real eigenvalues of the matrices $\mathbf{M}_f\mathbf{M}_f^{\dagger}$ and $\mathbf{M}_f^{\dagger}\mathbf{M}_f$. Therefore, from the expressions in Eq. (16), we obtain

$$\mathbf{V}_f\mathbf{M}_f\mathbf{U}_f^{\dagger} = \mathbf{\Delta}_{f,\Sigma}, \quad \text{or} \quad \mathbf{M}_f = \mathbf{V}_f^{\dagger}\mathbf{\Delta}_{f,\Sigma}\mathbf{U}_f, \tag{17}$$

where $\mathbf{\Delta}_{f,\Sigma} = \text{diag}\left(\Sigma_{f1}, \Sigma_{f2}, \Sigma_{f3}\right)$. The $\Sigma_{fi} \equiv \sqrt{\lambda_{fi}}$ are the singular values of the matrix $\mathbf{M}_f$, which may be complex quantities.

In order to determine the explicit form of the unitary matrices $\mathbf{U}_f$ and $\mathbf{V}_f$, we will consider two possible internal symmetries of the mass matrix $\mathbf{M}_f$. The first is to consider the mass matrix as a Hermitian matrix, and the second is to consider it as a complex symmetric matrix. In the case of representing the mass matrix through a Hermitian matrix, the condition $\mathbf{M}_f = \mathbf{M}_f^{\dagger}$ must be satisfied. Then, from Eq. (17), the self-adjoint matrix of the fermion mass matrix can be written as

$$\mathbf{M}_f^{\dagger} = \mathbf{U}_f^{\dagger}\,\mathbf{\Delta}_{f,\Sigma}^{\dagger}\,\mathbf{V}_f. \tag{18}$$

By comparing the matrices in Eqs. (17) and (18), it follows that the unitary matrices satisfy the relation $\mathbf{U}_f = \mathbf{V}_f$. Moreover, $\mathbf{\Delta}_{f,\Sigma} = \mathbf{\Delta}_{f,\Sigma}^{\dagger}$, which implies that the elements of the matrix $\mathbf{\Delta}_{f,\Sigma}$ are real quantities. Consequently, and in accordance with the singular value decomposition theorem, in this particular case the fermion mass matrix in Eq. (17) takes the form

$$\mathbf{M}_f = \mathbf{U}_f^{\dagger}\mathbf{\Delta}_{f,m}\mathbf{U}_f \quad \Rightarrow \quad \mathbf{U}_f\mathbf{M}_f\mathbf{U}_f^{\dagger} = \mathbf{\Delta}_{f,m}, \tag{19}$$

where $\mathbf{\Delta}_{f,m} = \text{diag}\left(m_{f1}, m_{f2}, m_{f3}\right)$. In this case, the singular values and the eigenvalues of the matrix $\mathbf{M}_f$ are equal. Therefore, the $m_{fi} = \Sigma_{fi}$ are the physical masses of the fermions.

On the other hand, when representing the fermion mass matrix through a complex symmetric mass matrix, the condition $\mathbf{M}_f = \mathbf{M}_f^{\top}$ must hold. Then, starting from Eq. (17), the transpose of the fermion mass matrix can be written as

$$\mathbf{M}_f^{\top} = \mathbf{U}_f^{\top}\,\mathbf{\Delta}_{f,\Sigma}^{\top}\,\mathbf{V}_f^{*}. \tag{20}$$

By comparing the matrices in Eqs. (17) and (20), it follows that the unitary matrices satisfy the relation $\mathbf{U}_f^{\top} = \mathbf{V}_f^{\dagger}$ or $\mathbf{U}_f = \mathbf{V}_f^{*}$. Furthermore, the relation $\mathbf{\Delta}_{f,\Sigma} = \mathbf{\Delta}_{f,\Sigma}^{\top}$ is automatically satisfied because the matrix $\mathbf{\Delta}_{f,\Sigma}$ is a diagonal matrix. Consequently, the fermion mass matrix in Eq. (17) takes the form

$$\mathbf{M}_f = \mathbf{U}_f^\top \mathbf{\Delta}_{f,\Sigma} \mathbf{U}_f. \tag{21}$$

In general, the elements of the matrix $\mathbf{\Delta}_{f,\Sigma}$ are complex quantities, so it can be written as

$$\mathbf{\Delta}_{f,\Sigma} = \mathbf{K}_f \mathbf{\Delta}_{f,m} \mathbf{K}_f, \tag{22}$$

where $\mathbf{\Delta}_{f,m} = \mathrm{diag}\,(m_{f1}, m_{f2}, m_{f3})$ and $\mathbf{K}_f = \mathrm{diag}\left(e^{i(\varphi_{f1}/2)}, e^{i(\varphi_{f2}/2)}, e^{i(\varphi_{f3}/2)}\right)$, with $m_{fi} = |\Sigma_{fi}|$ and $\varphi_{fi} = \arg\{m_{fi}\}$. From Eq. (22), the fermion mass matrix in equation (21) can be expressed as

$$\mathbf{M}_f = \mathcal{U}_f^\top \mathbf{\Delta}_{f,m} \mathcal{U}_f \quad \Rightarrow \quad \mathcal{U}_f^* \mathbf{M}_f \mathcal{U}_f^\dagger = \mathbf{\Delta}_{f,m}, \tag{23}$$

where $\mathcal{U}_f = \mathbf{K}_f \mathbf{U}_f$. The phase factors present in the diagonal matrix $\mathbf{K}_f$ can be absorbed into the spinors of the mass terms. It is common to associate these phase factors with the CP-violating phases of the Majorana type.

In summary, the mass matrices given in Eqs. (19) and (23) can be expressed in the following compact form:

$$\mathbb{V}_f^{\mathsf{j}}\, \mathbf{M}_f\, \mathbb{U}_f^{\mathsf{j}\dagger} = \mathbf{\Delta}_{f,m}, \qquad \mathsf{j} = 1, 2, \tag{24}$$

where

$$\begin{aligned} &\mathbb{U}_f^1 = \mathbf{U}_f, \quad \mathbb{V}_f^1 = \mathbf{U}_f, \quad \text{for} \quad \mathbf{M}_f = \mathbf{M}_f^\dagger, \\ &\mathbb{U}_f^2 = \mathcal{U}_f, \quad \mathbb{V}_f^2 = \mathcal{U}_f^*, \quad \text{for} \quad \mathbf{M}_f = \mathbf{M}_f^\top, \end{aligned} \tag{25}$$

with $\mathcal{U}_f = \mathbf{K}_f \mathbf{U}_f$.

3.1. Fermion mass matrix 3×3

The general fermion mass matrix of 3×3 can be written in the following expression:

$$\mathbf{M}_f = \begin{pmatrix} m_{11}^f & m_{12}^f & m_{13}^f \\ m_{21}^f & m_{22}^f & m_{23}^f \\ m_{31}^f & m_{32}^f & m_{33}^f \end{pmatrix}, \tag{26}$$

where the superscript $f = u, d, \ell, \nu$ denotes the up quarks, down quarks, charged leptons, and neutrinos, respectively. The elements m_{ij}^f of the matrix $\mathbf{M}_f$, with $i, j = 1, 2, 3$, are complex quantities. The fermion mass matrix $\mathbf{M}_f$ can be rotated via the orthogonal transformation

$$\mathbf{M}_{Rf} = \mathbf{R}_{\beta_f}\, \mathbf{M}_f\, \mathbf{R}_{\beta_f}^\top \quad \text{or} \quad \mathbf{M}_f = \mathbf{R}_{\beta_f}^\top\, \mathbf{M}_{Rf}\, \mathbf{R}_{\beta_f}. \tag{27}$$

In these expressions, $\mathbf{R}_{\beta_f}$ is a real symmetric rotation matrix given as

$$\mathbf{R}_{\beta_f} = \begin{pmatrix} 1 & 0 & 0 \\ 0 & \cos\beta_f & \sin\beta_f \\ 0 & -\sin\beta_f & \cos\beta_f \end{pmatrix}. \tag{28}$$

On the other hand, in order to generate a zero in the $(1,3)$ entry of the matrix $\mathbf{M}_{Rf}$, it is required that the relation

$$\tan\beta_f = \frac{m_{13}^f}{m_{12}^f}, \tag{29}$$

whereas, to generate a zero in the $(3,1)$ entry of the matrix $\mathbf{M}_{Rf}$, the relation must be hold

$$\tan\beta_f = \frac{m_{31}^f}{m_{21}^f}. \tag{30}$$

By comparing the expressions in Eqs. (29) and (30), it can be observed that both refer to the same rotation angle β_f, and therefore, the relation

$$\frac{m_{13}^f}{m_{12}^f} = \frac{m_{31}^f}{m_{21}^f}. \tag{31}$$

In order for the definition of the angle β_f to be a real quantity, and corresponds to a pure rotation, the relation must hold

$$\begin{aligned} \arg\left\{m_{13}^f\right\} &= \arg\left\{m_{31}^f\right\}, \\ \arg\left\{m_{21}^f\right\} &= \arg\left\{m_{12}^f\right\}. \end{aligned} \tag{32}$$

Thus, the rotated mass matrix, $\mathbf{M}_{Rf}$, takes the form

$$\mathbf{M}_{Rf} = \begin{pmatrix} m_{11}^f & A_f & 0 \\ A'_f & B'_f & C_f \\ 0 & C'_f & D'_f \end{pmatrix}, \tag{33}$$

here in the following expressions $t_{\beta_f} \equiv \tan\beta_f$,

$$\begin{aligned} A_f &= m_{12}^f\sqrt{1 + t_{\beta_f}^2}, \quad A'_f = m_{21}^f\sqrt{1 + t_{\beta_f}^2}, \\ B'_f &= \frac{m_{22} + m_{33}t_{\beta_f}^2 + (m_{23} + m_{32})\, t_{\beta_f}}{1 + t_{\beta_f}^2}, \\ C_f &= \frac{m_{23} - m_{32}t_{\beta_f}^2 + (m_{33} - m_{22})\, t_{\beta_f}}{1 + t_{\beta_f}^2}, \\ C'_f &= \frac{m_{32} - m_{23}t_{\beta_f}^2 + (m_{33} - m_{22})\, t_{\beta_f}}{1 + t_{\beta_f}^2}, \\ D'_f &= \frac{m_{33} + m_{22}t_{\beta_f}^2 - (m_{23} + m_{32})\, t_{\beta_f}}{1 + t_{\beta_f}^2}. \end{aligned} \tag{34}$$

Motivated by the hierarchical pattern of fermion masses and mixings, where direct first–third family couplings are suppressed with respect to nearest–neighbour interactions, we work in an intermediate weak basis in which the $(1,3)$ and $(3,1)$ entries of the mass matrix vanish. Such a structure can arise from approximate flavour symmetries or from vacuum alignment conditions following the minimization of extended Higgs potentials. Exploiting weak–basis freedom, the fermion mass matrix is therefore cast into a canonical form with $M_{13} = M_{31} = 0$, which should be regarded as a basis choice rather than a dynamical texture assumption. Requiring this transformation to be implemented by a single real rotation leads to the consistency conditions in Eqs. (31) and (32), ensuring that both entries are simultaneously eliminated. The resulting matrix, given in Eq. (33), represents the most general mass matrix within this canonical class. The analysis is then performed in two complementary scenarios, Hermitian and complex symmetric mass matrices, corresponding to Dirac and Majorana fermion mass terms, respectively. The general Dirac mass matrices can be diagonalized through biunitary transformations, equivalently associated with the diagonalization of Hermitian mass combinations carrying the same physical content [1,13-26].

In this analysis of the mass matrices and flavor mixing, two possible internal symmetries in the fermion mass matrices will be considered. The first internal symmetry to consider is representing the fermion mass matrix as a Hermitian matrix, $\mathbf{M}_f = \mathbf{M}_f^{\dagger}$. An immediate consequence of this internal symmetry is that the rotated matrix satisfies $\mathbf{M}_{Rf} = \mathbf{M}_{Rf}^{\dagger}$. Thus, the elements of the matrix $\mathbf{M}_{Rf}$ fulfill the relations $A_f' = A_f^*$, $C_f' = C_f^*$, $B_f' = B_f^{'*}$, and $D_f' = D_f^{'*}$. From the previous expressions, it can be concluded that the diagonal elements are real quantities, $m_{11}^f = m_{11}^{f*}$, $m_{22}^f = m_{22}^{f*}$, $m_{33}^f = m_{33}^{f*}$, and that the off-diagonal elements satisfy $m_{21}^f = m_{12}^{f*}$, $m_{31}^f = m_{13}^{f*}$, $m_{32}^f = m_{23}^{f*}$. The second internal symmetry that will be considered here is to treat the fermion mass matrix as a complex symmetric matrix, $\mathbf{M}_f = \mathbf{M}_f^{\top}$. An immediate consequence of the previous symmetry is that the rotated matrix satisfies the relation $\mathbf{M}_{Rf} = \mathbf{M}_{Rf}^{\top}$. Therefore, the elements of this matrix satisfy $A_f' = A_f$ and $C_f' = C_f$. Additionally, the off-diagonal elements of the matrix $\mathbf{M}_f$ satisfy the conditions $m_{12}^f = m_{21}^f$, $m_{13}^f = m_{31}^f$, $m_{23}^f = m_{32}^f$.

The matrix $\mathbf{M}_{Rf}$ can be expressed in polar form, therefore,

$$\mathbf{M}_{Rf} = \mathbf{Q}_f \, \bar{\mathbf{M}}_{Rf} \, \mathbf{P}_f, \tag{35}$$

where $\mathbf{Q}_f = \mathbf{P}_f^{\dagger}$ for the case when $\mathbf{M}_f$ is Hermitian, and $\mathbf{Q}_f = \mathbf{P}_f^{\top}$ for when $\mathbf{M}_f$ is a complex symmetric matrix. The explicit form of the phase factor matrix is

$$\begin{aligned}
\mathbf{P}_f &= \mathrm{diag}\left\{1, e^{i\vartheta_{f,a}}, e^{i(\vartheta_{f,c}+\vartheta_{f,a})}\right\} \text{ for } \mathbf{M}_f = \mathbf{M}_f^{\dagger}, \\
\mathbf{P}_f &= \mathrm{diag}\left\{1, e^{i\vartheta_{f,a}}, e^{i(\vartheta_{f,c}-\vartheta_{f,a})}\right\} \text{ for } \mathbf{M}_f = \mathbf{M}_f^{\top},
\end{aligned} \tag{36}$$

where $\vartheta_{f,a} = \arg\{A_f\}$ and $\vartheta_{f,c} = \arg\{C_f\}$. Additionally, for the case $\mathbf{M}_f = \mathbf{M}_f^{\top}$, the following relations must hold: $\arg\{B_f\} = 2\arg\{A_f\}$ and $\arg\{D_f\} = 2\left(\arg\{C_f\} - \arg\{A_f\}\right)$. The real symmetric matrix, $\bar{\mathbf{M}}_{Rf}$, can be written as

$$\bar{\mathbf{M}}_{Rf} = m_{11}^f \mathbb{I}_{3\times3} + \mathcal{M}_f, \tag{37}$$

where $\mathbb{I}_{3\times3} = \mathrm{diag}\,(1,1,1)$,

$$\mathcal{M}_f = \begin{pmatrix} 0 & \mathcal{A}_f & 0 \\ \mathcal{A}_f & \mathcal{B}_f & \mathcal{C}_f \\ 0 & \mathcal{C}_f & \mathcal{D}_f \end{pmatrix}, \tag{38}$$

where for both internal symmetries in the fermion mass matrix, it holds that $\mathcal{A}_f = |A_f|$, $\mathcal{B}_f = B_f$, $\mathcal{C}_f = |C_f|$, $\mathcal{D}_f = D_f$. For a Hermitian mass matrix $\mathbf{M}_f$,

$$\begin{aligned}
\mathcal{A}_f &= |m_{12}^f|\sqrt{1+t_{\beta_f}^2}, \\
\mathcal{B}_f &= \frac{m_{22} + m_{33}t_{\beta_f}^2 + (m_{23}+m_{23}^*)\,t_{\beta_f}}{1+t_{\beta_f}^2} - m_{11}^f, \\
\mathcal{C}_f &= \left|\frac{m_{23} - m_{23}^* t_{\beta_f}^2 + (m_{33}-m_{22})\,t_{\beta_f}}{1+t_{\beta_f}^2}\right|, \\
\mathcal{D}_f &= \frac{m_{33} + m_{22}t_{\beta_f}^2 - (m_{23}+m_{23}^*)\,t_{\beta_f}}{1+t_{\beta_f}^2} - m_{11}^f.
\end{aligned} \tag{39}$$

On the other hand, a complex symmetric mass matrix $\mathbf{M}_f$,

$$\begin{aligned}
\mathcal{A}_f &= |m_{12}^f|\sqrt{1+t_{\beta_f}^2}, \\
\mathcal{B}_f &= \left|\frac{m_{22} + m_{33}t_{\beta_f}^2 + 2m_{23}t_{\beta_f}}{1+t_{\beta_f}^2}\right| - m_{11}^f, \\
\mathcal{C}_f &= \left|\frac{m_{23}\left(1-t_{\beta_f}^2\right) + (m_{33}-m_{22})\,t_{\beta_f}}{1+t_{\beta_f}^2}\right|, \\
\mathcal{D}_f &= \left|\frac{m_{33} + m_{22}t_{\beta_f}^2 - 2m_{23}t_{\beta_f}}{1+t_{\beta_f}^2}\right| - m_{11}^f.
\end{aligned} \tag{40}$$

Without loss of generality, here m_{11}^f is considered a real quantity. This is possible because the matrix $\mathbf{P}_f$ always allows a phase factor to be factored out, which would be absorbed by the spinors of the mass term. With the help of the expressions in Eqs. (35) and (37), the mass matrix in Eq. (27) can be rewritten as

$$\mathbf{M}_f = \mathbf{R}_{\beta_f}^{\top}\mathbf{Q}_f\left(m_{11}^f \mathbb{I}_{3\times3} + \mathcal{M}_f\right)\mathbf{P}_f\mathbf{R}_{\beta_f}. \tag{41}$$

The real symmetric matrix $\mathcal{M}_f$ can be diagonalized through the following orthogonal transformation

$$\mathcal{M}_f = \mathbf{O}_f \mathbf{\Delta}_{f,\sigma} \mathbf{O}_f^{\top}, \tag{42}$$

where $\mathbf{\Delta}_{f,\sigma} = \mathrm{diag}\,(\sigma_{f1}, \sigma_{f2}, \sigma_{f3})$, here the σ_{fi} are the eigenvalues of the real symmetric matrix $\mathcal{M}_f$ and are known as the running masses of the fermions [27]. Thus,

$$\mathbf{M}_f = \mathbf{R}_{\beta_f}^{\top}\mathbf{Q}_f\mathbf{O}_f\left(m_{11}^f \mathbb{I}_{3\times3} + \mathbf{\Delta}_{f,\sigma}\right)\mathbf{O}_f^{\top}\mathbf{P}_f\mathbf{R}_{\beta_f}. \tag{43}$$

From the above mass matrix, Eq. (43), for the quark sector when the mass matrix is represented by a Hermitian matrix, it takes the form

$$\mathbf{M}_q = \mathbf{U}_q^{\dagger}\mathbf{\Delta}_{q,m}\mathbf{U}_q, \tag{44}$$

where $q = u, d$ denotes the up-type and down-type quarks, and $\mathbf{U}_q = \mathbf{O}_q^\top \mathbf{P}_q \mathbf{R}_{\beta_q}$ is the unitary matrix that diagonalizes the quark mass matrix. While in the case when the quark mass matrix is represented by a complex symmetric matrix, we have

$$\mathbf{M}_q = \mathbf{U}_q^\top \boldsymbol{\Delta}_{q,m} \mathbf{U}_q, \tag{45}$$

with $q = u, d$ denotes the up-type and down-type quarks, and $\mathbf{U}_q = \mathbf{O}_q^\top \mathbf{P}_q \mathbf{R}_{\beta_q}$ is the unitary matrix that diagonalizes the quark mass matrix. Furthermore, in the previous expressions $\boldsymbol{\Delta}_{q,m} = \text{diag}\,(m_{q1}, m_{q2}, m_{q3})$ is a diagonal matrix of the physical masses of the quarks.

In contrast, for the lepton sector when the mass matrix is represented by a Hermitian matrix, the expression in Eq. (43) can be rewritten as

$$\mathbf{M}_l = \mathbf{U}_l \boldsymbol{\Delta}_{l,m} \mathbf{U}_l^\dagger, \tag{46}$$

where $l = \ell, \nu$ denotes the charged leptons and neutrinos. Furthermore, $\mathbf{U}_l = \mathbf{R}_{\beta_l}^\top \mathbf{P}_l^\dagger \mathbf{O}_l$ is the unitary matrix that diagonalizes the lepton mass matrix. For the case when the lepton mass matrix is represented by a complex symmetric matrix,

$$\mathbf{M}_l = \mathbf{U}_l \boldsymbol{\Delta}_{l,m} \mathbf{U}_l^\top, \tag{47}$$

where $l = \ell, \nu$ denotes the charged leptons and neutrinos. Additionally, $\mathbf{U}_l = \mathbf{R}_{\beta_l}^\top \mathbf{P}_l^\top \mathbf{O}_l$ is the unitary matrix that diagonalizes the lepton mass matrix. Thus, in the previous expressions, $\boldsymbol{\Delta}_{l,m} = \text{diag}\,(m_{l1}, m_{l2}, m_{l3})$ is a diagonal matrix of the physical masses of the leptons.

The hierarchy between fermionic masses is taken into account considering the normal hierarchy (NH), it is assumed that the first two fermions have small masses and are closer to each other, while the third is considerably heavier.

$$m_{f,1} < m_{f,2} \ll m_{f,3}, \text{with} f = l, \nu. \tag{48}$$

In the inverted hierarchy (IH), consistent just with neutrinos, the two heavier fermions are nearly degenerate, while the third is considerably lighter. In terms of the mass differences:

$$m_{\nu 3} \ll m_{\nu 1} < m_{\nu 2}. \tag{49}$$

Despite his scenario is less intuitive as NH, it is compatible with the experimental data available so far. It has not yet been confirmed which of the two mass hierarchies is correct, but future experiments such as DUNE (Deep Underground Neutrino Experiment) [28] and JUNO (Jiangmen Underground Neutrino Observatory) aim to determine the neutrino hierarchy as one of their main objectives.

From the expression in Eq. (43), we obtain

$$\sigma_{fi} = \mathsf{s}_i m_{fi} - m_{11}^f, \tag{50}$$

which relates the physical masses of the fermions with their running masses. In this expression, the s_i $(i = 1, 2, 3)$ is a sign that take values ± 1, such that $\mathcal{A}_f^2 \geq 0$ is guaranteed. Changing the sign of one of the eigenvalues is equivalent to performing a rotation in the eigenvalue space. In other words, for fermion fields, the sign of the mass is irrelevant, as the sign can be changed via a chiral transformation: $f_R \to f_R' = e^{i\gamma_5(\pi/2)} f_R$ and $f_L \to f_L' = e^{i\gamma_5(\pi/2)} f_L$. These transformations change the sign of the eigenvalues, but leave invariant the rest of the Lagrangian.

4. Orthogonal matrix in terms of the fermion masses

The square of the matrix $\mathcal{M}_f$ is

$$\mathcal{M}_f^2 = \mathcal{M}_f^\dagger \mathcal{M}_f = \begin{pmatrix} \mathcal{A}_f^2 & \mathcal{A}_f \mathcal{B}_f & \mathcal{A}_f \mathcal{C}_f \\ \mathcal{A}_f \mathcal{B}_f & \mathcal{A}_f^2 + \mathcal{B}_f^2 + \mathcal{C}_f^2 & \mathcal{B}_f \mathcal{C}_f + \mathcal{C}_f \mathcal{D}_f \\ \mathcal{A}_f \mathcal{C}_f & \mathcal{B}_f \mathcal{C}_f + \mathcal{C}_f \mathcal{D}_f & \mathcal{C}_f^2 + \mathcal{D}_f^2 \end{pmatrix}. \tag{51}$$

Therefore, $\mathcal{M}_f^2 = \mathbf{O}_f^\top \boldsymbol{\Delta}_{f,\sigma}^2 \mathbf{O}_f$ where $\boldsymbol{\Delta}_{f,\sigma}^2 = \text{diag}\left(\sigma_{f1}^2, \sigma_{f2}^2, \sigma_{f3}^2\right)$. The invariants of the matrix $\mathcal{M}_f$ satisfy the relations

$$\begin{aligned} &\text{Tr}\,\{\mathcal{M}_f\} = \text{Tr}\,\{\boldsymbol{\Delta}_{f,\sigma}\} \Rightarrow \mathcal{B}_f + \mathcal{D}_f = \sigma_{f1} + \sigma_{f2} + \sigma_{f3}, \\ &\det\{\mathcal{M}_f\} = \det\{\boldsymbol{\Delta}_{f,\sigma}\} \Rightarrow -\mathcal{A}_f^2 \mathcal{D}_f = \sigma_{f1}\sigma_{f2}\sigma_{f3}, \\ &\chi\,\{\mathcal{M}_f\} = \frac{1}{2}\left(\text{Tr}\,\{\mathcal{M}_f^2\} - \text{Tr}\,\{\mathcal{M}_f\}^2\right), \\ &\mathcal{A}_f^2 - \mathcal{B}_f \mathcal{D}_f + \mathcal{C}_f^2 = -\sigma_{f1}\sigma_{f2} - \sigma_{f1}\sigma_{f3} - \sigma_{f2}\sigma_{f3}. \end{aligned} \tag{52}$$

Thus, the elements of the real symmetric matrix $\mathcal{M}_f$ in terms of the running masses of the fermions take the form

$$\mathcal{A}_f = \sqrt{\frac{\sigma_{f1}\sigma_{f2}\sigma_{f3}}{\mathcal{D}_f}}, \tag{53a}$$

$$\mathcal{B}_f = \mathsf{s}_3 \sigma_{f3} + \mathsf{s}_2 \sigma_{f2} + \mathsf{s}_1 \sigma_{f1} - \mathcal{D}_f, \tag{53b}$$

$$\mathcal{C}_f = \sqrt{\frac{(\mathsf{s}_3\sigma_{f3} - \mathcal{D}_f)(\mathcal{D}_f - \mathsf{s}_2\sigma_{f2})(\mathcal{D}_f - \mathsf{s}_1\sigma_{f1})}{\mathcal{D}_f}}. \tag{53c}$$

The parameters m_{11}^f and $\mathcal{D}_f$ must satisfy the conditions:

For a normal hierarchy in the fermion mass spectrum: $\sigma_{f3} > \sigma_{f2} > \sigma_{f1}$

$$
\begin{array}{llll}
m_{f1} > m_{11}^{f}, & & & \\
\sigma_{f3} > \mathcal{D}_f > \sigma_{f2}, & \mathcal{D}_f \neq -\sigma_{f1} + \sigma_{f2} + \sigma_{f3}, & \text{for} \quad m_{f1} \to -|m_{f1}|, & \mathsf{s}_1 = -1,\ \mathsf{s}_2 = +1,\ \mathsf{s}_3 = +1, \\
\sigma_{f3} > \mathcal{D}_f > \sigma_{f1}, & \mathcal{D}_f \neq +\sigma_{f1} - \sigma_{f2} + \sigma_{f3}, & \text{for} \quad m_{f2} \to -|m_{f2}|, & \mathsf{s}_1 = +1,\ \mathsf{s}_2 = -1,\ \mathsf{s}_3 = +1, \\
\sigma_{f2} > \mathcal{D}_f > \sigma_{f1}, & \mathcal{D}_f \neq +\sigma_{f1} + \sigma_{f2} - \sigma_{f3}, & \text{for} \quad m_{f3} \to -|m_{f3}|, & \mathsf{s}_1 = +1,\ \mathsf{s}_2 = +1,\ \mathsf{s}_3 = -1.
\end{array}
\tag{54}
$$

For an inverted hierarchy in the fermion mass spectrum:
$\sigma_{f2} > \sigma_{f1} > \sigma_{f3}$

$$
\begin{array}{llll}
m_{f3} > m_{11}^{f}, & & & \\
\sigma_{f2} > \mathcal{D}_f > \sigma_{f3}, & \mathcal{D}_f \neq -\sigma_{f1} + \sigma_{f2} + \sigma_{f3}, & \text{for} \quad m_{f1} \to -m_{f1}, & \mathsf{s}_1 = -1,\ \mathsf{s}_2 = +1,\ \mathsf{s}_3 = +1, \\
\sigma_{f1} > \mathcal{D}_f > \sigma_{f3}, & \mathcal{D}_f \neq +\sigma_{f1} - \sigma_{f2} + \sigma_{f3}, & \text{for} \quad m_{f2} \to -m_{f2}, & \mathsf{s}_1 = +1,\ \mathsf{s}_2 = -1,\ \mathsf{s}_3 = +1, \\
\sigma_{f2} > \mathcal{D}_f > \sigma_{f1}, & \mathcal{D}_f \neq +\sigma_{f1} + \sigma_{f2} - \sigma_{f3}, & \text{for} \quad m_{f3} \to -m_{f3}, & \mathsf{s}_1 = +1,\ \mathsf{s}_2 = +1,\ \mathsf{s}_3 = -1.
\end{array}
\tag{55}
$$

In agreement with experimental data on neutrino oscillations, the inverted hierarchy is only present in the neutrino mass spectrum.

The real symmetric matrix $\mathcal{M}_f$ can be brought to its diagonal form by means of the orthogonal transformation in Eq. (42). The orthogonal matrix $\mathbf{O}_f$ is constructed using the eigenvectors of the matrix $\mathcal{M}_f$, and it has the following expression:

$$
\mathbf{O}_f = \left(\mathsf{s}_1 |M_1\rangle, \mathsf{s}_2 |M_2\rangle, \mathsf{s}_3 |M_3\rangle\right). \tag{56}
$$

The form of the eigenvector for a general matrix $\mathbf{M}_f$, Eq. (26), is [29]:

$$
|M_k\rangle = \frac{1}{N_i} \begin{pmatrix} (\lambda_i - m_{22})\, m_{13} + m_{12} m_{23} \\ (\lambda_i - m_{11})\, m_{23} + m_{21} m_{13} \\ (\lambda_i - m_{11})\,(\lambda_i - m_{22}) - m_{12} m_{21} \end{pmatrix}. \tag{57}
$$

In this expression, λ_i ($i = 1, 2, 3$) correspond to the eigenvalues of the matrix $\mathbf{M}_f$, and $N_i \equiv \sqrt{\langle \mathbf{M}_i | \mathbf{M}_i \rangle}$ are the normalization constants. The orthogonal matrix $\mathbf{O}_f$ that diagonalizes the mass matrix $\mathcal{M}_f$ takes the expression

$$
\begin{pmatrix}
\mathsf{s}_1 \sqrt{\frac{\sigma_{f2}\sigma_{f3}\xi_{f1}}{\mathsf{D}_{f1}}} & \mathsf{s}_2 \sqrt{\frac{\sigma_{f1}\sigma_{f3}\xi_{f2}}{\mathsf{D}_{f2}}} & \mathsf{s}_3 \sqrt{\frac{\sigma_{f1}\sigma_{f2}\xi_{f3}}{\mathsf{D}_{f3}}} \\
\sqrt{\frac{\sigma_{f1}\mathcal{D}_f\xi_{f1}}{\mathsf{D}_{f1}}} & \sqrt{\frac{\sigma_{f2}\mathcal{D}_f\xi_{f2}}{\mathsf{D}_{f2}}} & \sqrt{\frac{\sigma_{f3}\mathcal{D}_f\xi_{f3}}{\mathsf{D}_{f3}}} \\
-\sqrt{\frac{\sigma_{f1}\xi_{f3}\xi_{f2}}{\mathsf{D}_{f1}}} & \mathsf{s}_1\mathsf{s}_2 \sqrt{\frac{\sigma_{f2}\xi_{f3}\xi_{f1}}{\mathsf{D}_{f2}}} & \mathsf{s}_3 \sqrt{\frac{\sigma_{f3}\xi_{f1}\xi_{f2}}{\mathsf{D}_{f3}}}
\end{pmatrix}, \tag{58}
$$

where $\sigma_{f1} = \mathsf{s}_1 m_{f1} - m_{11}^{f}$, $\sigma_{f2} = \mathsf{s}_2 m_{f2} - m_{11}^{f}$, $\sigma_{f3} = \mathsf{s}_3 m_{f3} - m_{11}^{f}$, $\xi_{f1} = (\mathcal{D}_f - \mathsf{s}_1\sigma_{f1})$, $\xi_{f2} = \mathsf{s}_3\,(\mathcal{D}_f - \mathsf{s}_2\sigma_{f2})$, $\xi_{f3} = (\sigma_{f3} - \mathsf{s}_3\mathcal{D}_f)$,

$$
\begin{aligned}
\mathsf{D}_{f1} &= \mathcal{D}_f\,(\sigma_{f2} + \mathsf{s}_3\sigma_{f1})\,(\sigma_{f3} + \mathsf{s}_2\sigma_{f1}), \\
\mathsf{D}_{f2} &= \mathcal{D}_f\,(\sigma_{f3} + \mathsf{s}_1\sigma_{f2})\,(\sigma_{f2} + \mathsf{s}_3\sigma_{f1}), \\
\mathsf{D}_{f3} &= \mathcal{D}_f\,(\sigma_{f3} + \mathsf{s}_1\sigma_{f2})\,(\sigma_{f3} + \mathsf{s}_2\sigma_{f1}).
\end{aligned}
\tag{59}
$$

5. Lepton flavor mixing matrix

In this case, the unitary matrix that diagonalizes the mass matrix of the leptons takes the form

$$
\begin{aligned}
\mathbf{U}_l &= \mathbf{R}_{\beta_l}^{\top}\mathbf{P}_l^{\dagger}\mathbf{O}_l, \quad \text{for} \quad \mathbf{M}_l = \mathbf{M}_l^{\dagger}, \\
\mathbf{U}_l &= \mathbf{R}_{\beta_l}^{\top}\mathbf{P}_l^{\top}\mathbf{O}_l, \quad \text{for} \quad \mathbf{M}_l = \mathbf{M}_l^{\top}.
\end{aligned}
\tag{60}
$$

Therefore, the lepton flavor mixing matrix, PMNS, which is defined as $\mathbf{V}_{\text{PMNS}} = \mathbf{U}_\ell^{\dagger}\mathbf{U}_\nu$ [1], takes the form

$$
\begin{aligned}
\mathbf{V}_{\text{PMNS}} &= \mathbf{O}_\ell^{\top}\mathbf{P}_\ell\mathbf{R}_{\beta_{\ell\nu}}\mathbf{P}_\nu^{\dagger}\mathbf{O}_\nu, \quad \text{for} \quad \mathbf{M}_l = \mathbf{M}_l^{\dagger}, \\
\mathbf{V}_{\text{PMNS}} &= \mathbf{O}_\ell^{\top}\mathbf{P}_\ell^{\dagger}\mathbf{R}_{\beta_{\ell\nu}}\mathbf{P}_\nu\mathbf{O}_\nu, \quad \text{for} \quad \mathbf{M}_l = \mathbf{M}_l^{\top}.
\end{aligned}
\tag{61}
$$

In the above expressions, we have

$$
\mathbf{R}_{\beta_{ud}} = \begin{pmatrix} 1 & 0 & 0 \\ 0 & \cos(\beta_\ell - \beta_\nu) & \sin(\beta_\ell - \beta_\nu) \\ 0 & -\sin(\beta_\ell - \beta_\nu) & \cos(\beta_\ell - \beta_\nu) \end{pmatrix}. \tag{62}
$$

In the particular case when the rotation angle is the same in both lepton sectors, $\beta_\ell = \beta_\nu$, the matrices in Eq. (61) take the form

$$
\mathbf{V}_{\text{PMNS}} = \mathbf{O}_\ell^{\top}\mathbf{P}_{\ell\nu}\mathbf{O}_\nu, \tag{63}
$$

where $\mathbf{P}_{\ell\nu} = \mathbf{P}_\ell\mathbf{P}_\nu^{\dagger}$ for $\mathbf{M}_l = \mathbf{M}_l^{\dagger}$, while $\mathbf{P}_{\ell\nu} = \mathbf{P}_\ell^{\dagger}\mathbf{P}_\nu$ for $\mathbf{M}_l = \mathbf{M}_l^{\top}$. In explicit form

$$
\begin{aligned}
\mathbf{P}_{\ell\nu} &= \text{diag}\left(1, e^{i\Phi_a}, e^{i\Phi_c}\right) \quad \text{for} \quad \mathbf{M}_l = \mathbf{M}_l^{\dagger}, \\
\mathbf{P}_{\ell\nu} &= \text{diag}\left(1, e^{i\Phi_a}, e^{i\Phi_c}\right) \quad \text{for} \quad \mathbf{M}_l = \mathbf{M}_l^{\top}.
\end{aligned}
\tag{64}
$$

Here, $\Phi_a = \vartheta_{\ell,a} - \vartheta_{\nu,a}$ and $\Phi_c = \vartheta_{\ell,c} - \vartheta_{\nu,c}$ for $\mathbf{M}_l = \mathbf{M}_l^{\dagger}$, and $\Phi_a = \vartheta_{\nu,a} - \vartheta_{\ell,a}$ and $\Phi_c = \vartheta_{\nu,c} - \vartheta_{\ell,c}$ for $\mathbf{M}_l = \mathbf{M}_l^{\top}$.

The difference between representing the mass matrix of the leptons with a Hermitian matrix or with a complex symmetric matrix mainly lies in the diagonal phase factor matrix $\mathbf{P}_{ud}$. However, as the lepton flavor mixing matrix PMNS is defined in Eq. (63), it is not possible to obtain direct information about whether the mass matrix is complex symmetric or Hermitian.

The values of the mass ratios of the quarks are more stable with respect to changes in the energy scale than the masses of the quarks themselves. In other words, the value of the mass ratios of the quarks has the same order of magnitude regardless of the energy scale [27,30]. In this work, the mass matrices, as well as the PMNS flavor mixing matrix, are normalized with respect to the masses of the heavier leptons. The charged leptons are normalized with respect to m_τ, obtaining $\widetilde{\sigma}_e = \widetilde{m}_e - \widetilde{m}^{\ell}_{11}$, $\widetilde{\sigma}_\mu = \widetilde{m}_\mu + \widetilde{m}^{\ell}_{11}$, $\widetilde{\sigma}_\tau = 1 - \widetilde{m}^{\ell}_{11}$, $\widetilde{\xi}_{\ell 1} = \widetilde{\mathcal{D}}_\ell - \widetilde{\sigma}_e$, $\widetilde{\xi}_{\ell 2} = \widetilde{\mathcal{D}}_\ell + \widetilde{\sigma}_\mu$, $\widetilde{\xi}_{\ell 3} = \widetilde{\sigma}_\tau - \widetilde{\mathcal{D}}_\ell$,

$$
\begin{aligned}
\widetilde{\mathsf{D}}_{\ell 1} &= \widetilde{\mathcal{D}}_\ell \left(\widetilde{\sigma}_\mu + \widetilde{\sigma}_e\right)\left(\widetilde{\sigma}_\tau - \widetilde{\sigma}_e\right),\\
\widetilde{\mathsf{D}}_{\ell 2} &= \widetilde{\mathcal{D}}_\ell \left(\widetilde{\sigma}_\tau + \widetilde{\sigma}_\mu\right)\left(\widetilde{\sigma}_\mu + \widetilde{\sigma}_e\right),\\
\widetilde{\mathsf{D}}_{\ell 3} &= \widetilde{\mathcal{D}}_\ell \left(\widetilde{\sigma}_\tau + \widetilde{\sigma}_\mu\right)\left(\widetilde{\sigma}_\tau - \widetilde{\sigma}_e\right),
\end{aligned}
\tag{65}
$$

where $\widetilde{m}_e = m_e/m_\tau$, $\widetilde{m}_\mu = m_\mu/m_\tau$, $\widetilde{m}^{\ell}_{11} = m^{\ell}_{11}/m_\tau$, $\widetilde{\sigma}_e = \sigma_e/m_\tau$, $\widetilde{\sigma}_\mu = \sigma_\mu/m_\tau$, $\widetilde{\sigma}_\tau = \sigma_\tau/m_\tau$, $\widetilde{\xi}_{\ell 1} = \xi_{\ell 1}/m_\tau$, $\widetilde{\xi}_{\ell 2} = \xi_{\ell 2}/m_\tau$, $\widetilde{\xi}_{\ell 3} = \xi_{\ell 3}/m_\tau$, $\widetilde{\mathcal{D}}_\ell = \mathcal{D}_\ell/m_\tau$. In the case of neutrinos with a normal hierarchy, $m_{\nu 3} > m_{\nu 2} > m_{\nu 1}$, in the mass spectrum we have $\widetilde{\sigma}_{\nu 1} = \widetilde{m}_{\nu 1} - \widetilde{m}^{\nu}_{11}$, $\widetilde{\sigma}_{\nu 2} = \widetilde{m}_{\nu 2} + \widetilde{m}^{\nu}_{11}$, $\widetilde{\sigma}_{\nu 3} = 1 - \widetilde{m}^{\nu}_{11}$, $\widetilde{\xi}_{\nu 1} = \widetilde{\mathcal{D}}_\nu - \widetilde{\sigma}_{\nu 1}$, $\widetilde{\xi}_{\nu 2} = \widetilde{\mathcal{D}}_\nu + \widetilde{\sigma}_{\nu 2}$, $\widetilde{\xi}_{\nu 3} = \widetilde{\sigma}_{\nu 3} - \widetilde{\mathcal{D}}_\nu$,

$$
\begin{aligned}
\widetilde{\mathsf{D}}_{\nu 1} &= \widetilde{\mathcal{D}}_\nu \left(\widetilde{\sigma}_{\nu 2} + \widetilde{\sigma}_{\nu 1}\right)\left(\widetilde{\sigma}_{\nu 3} - \widetilde{\sigma}_{\nu 1}\right),\\
\widetilde{\mathsf{D}}_{\nu 2} &= \widetilde{\mathcal{D}}_\nu \left(\widetilde{\sigma}_{\nu 3} + \widetilde{\sigma}_{\nu 2}\right)\left(\widetilde{\sigma}_{\nu 2} + \widetilde{\sigma}_{\nu 1}\right),\\
\widetilde{\mathsf{D}}_{\nu 3} &= \widetilde{\mathcal{D}}_\nu \left(\widetilde{\sigma}_{\nu 3} + \widetilde{\sigma}_{\nu 2}\right)\left(\widetilde{\sigma}_{\nu 3} - \widetilde{\sigma}_{\nu 1}\right),
\end{aligned}
\tag{66}
$$

where $\widetilde{m}_{\nu 1} = m_{\nu 1}/m_{\nu 3}$, $\widetilde{m}_{\nu 2} = m_{\nu 2}/m_{\nu 3}$, $\widetilde{m}^{\nu}_{11} = m^{\nu}_{11}/m_{\nu 3}$, $\widetilde{\sigma}_{\nu 1} = \sigma_{\nu 1}/m_{\nu 3}$, $\widetilde{\sigma}_{\nu 2} = \sigma_{\nu 2}/m_{\nu 3}$, $\widetilde{\sigma}_{\nu 3} = \sigma_{\nu 3}/m_{\nu 3}$, $\widetilde{\xi}_{\nu 1} = \xi_{\nu 1}/m_{\nu 3}$, $\widetilde{\xi}_{\nu 2} = \xi_{\nu 2}/m_{\nu 3}$, $\widetilde{\xi}_{\nu 3} = \xi_{\nu 3}/m_{\nu 3}$, and $\widetilde{\mathcal{D}}_\nu = \mathcal{D}_\nu/m_{\nu 3}$. In the case of neutrinos with an inverted hierarchy, $m_{\nu 2} > m_{\nu 1} > m_{\nu 3}$, in the mass spectrum we have $\widetilde{\sigma}_{\nu 1} = \widetilde{m}_{\nu 1} - \widetilde{m}^{\nu}_{11}$, $\widetilde{\sigma}_{\nu 2} = 1 + \widetilde{m}^{\nu}_{11}$, $\widetilde{\xi}_{\nu 1} = \widetilde{\mathcal{D}}_\nu - \widetilde{\sigma}_{\nu 1}$, $\widetilde{\sigma}_{\nu 3} = \widetilde{m}_{\nu 3} - \widetilde{m}^{\nu}_{11}$, $\widetilde{\xi}_{\nu 2} = \widetilde{\mathcal{D}}_\nu + \widetilde{\sigma}_{\nu 2}$, $\widetilde{\xi}_{\nu 3} = \widetilde{\sigma}_{\nu 3} - \widetilde{\mathcal{D}}_\nu$,

$$
\begin{aligned}
\widetilde{\mathsf{D}}_{\nu 1} &= \widetilde{\mathcal{D}}_\nu \left(\widetilde{\sigma}_{\nu 2} + \widetilde{\sigma}_{\nu 1}\right)\left(\widetilde{\sigma}_{\nu 3} - \widetilde{\sigma}_{\nu 1}\right),\\
\widetilde{\mathsf{D}}_{\nu 2} &= \widetilde{\mathcal{D}}_\nu \left(\widetilde{\sigma}_{\nu 3} + \widetilde{\sigma}_{\nu 2}\right)\left(\widetilde{\sigma}_{\nu 2} + \widetilde{\sigma}_{\nu 1}\right),\\
\widetilde{\mathsf{D}}_{\nu 3} &= \widetilde{\mathcal{D}}_\nu \left(\widetilde{\sigma}_{\nu 3} + \widetilde{\sigma}_{\nu 2}\right)\left(\widetilde{\sigma}_{\nu 3} - \widetilde{\sigma}_{\nu 1}\right),
\end{aligned}
\tag{67}
$$

where $\widetilde{m}_{\nu 1} = m_{\nu 1}/m_{\nu 2}$, $\widetilde{m}_{\nu 3} = m_{\nu 3}/m_{\nu 2}$, $\widetilde{m}^{\nu}_{11} = m^{\nu}_{11}/m_{\nu 2}$, $\widetilde{\sigma}_{\nu 1} = \sigma_{\nu 1}/m_{\nu 2}$, $\widetilde{\sigma}_{\nu 2} = \sigma_{\nu 2}/m_{\nu 2}$, $\widetilde{\sigma}_{\nu 3} = \sigma_{\nu 3}/m_{\nu 2}$, $\widetilde{\xi}_{\nu 1} = \xi_{\nu 1}/m_{\nu 2}$, $\widetilde{\xi}_{\nu 2} = \xi_{\nu 2}/m_{\nu 2}$, $\widetilde{\xi}_{\nu 3} = \xi_{\nu 3}/m_{\nu 2}$, and $\widetilde{\mathcal{D}}_\nu = \mathcal{D}_\nu/m_{\nu 2}$. For the particular case of performing a chiral rotation on the second eigenvalue, $m_{f2} = -|m_{f2}|$, which implies that $\mathsf{s}_1 = +1$, $\mathsf{s}_2 = -1$ and $\mathsf{s}_3 = +1$, the PMNS matrix takes the form

$$
\mathbf{V}^{\rm th}_{\rm PMNS} = \begin{pmatrix} V^{\rm th}_{e1} & V^{\rm th}_{e2} & V^{\rm th}_{e3} \\ V^{\rm th}_{\mu 1} & V^{\rm th}_{\mu 2} & V^{\rm th}_{\mu 3} \\ V^{\rm th}_{\tau 1} & V^{\rm th}_{\tau 2} & V^{\rm th}_{\tau 3} \end{pmatrix},
\tag{68}
$$

The elements of the PMNS mixing matrix are expressed as

$$
\begin{aligned}
V^{\rm th}_{e1} &= \sqrt{\frac{\widetilde{\sigma}_\mu\widetilde{\sigma}_\tau\widetilde{\sigma}_{\nu 2}\widetilde{\sigma}_{\nu 3}\widetilde{\xi}_{\ell 1}\widetilde{\xi}_{\nu 1}}{\widetilde{\mathsf{D}}_{\ell 1}\widetilde{\mathsf{D}}_{\nu 1}}} + \sqrt{\frac{\widetilde{\sigma}_e\widetilde{\sigma}_{\nu 1}}{\widetilde{\mathsf{D}}_{\ell 1}\widetilde{\mathsf{D}}_{\nu 1}}}\left(\sqrt{\widetilde{\mathcal{D}}_\ell\widetilde{\mathcal{D}}_\nu\widetilde{\xi}_{\ell 1}\widetilde{\xi}_{\nu 1}}e^{i\Phi_a} + \sqrt{\widetilde{\xi}_{\ell 2}\widetilde{\xi}_{\ell 3}\widetilde{\xi}_{\nu 2}\widetilde{\xi}_{\nu 3}}e^{i\Phi_c}\right),\\
V^{\rm th}_{e2} &= -\sqrt{\frac{\widetilde{\sigma}_\mu\widetilde{\sigma}_\tau\widetilde{\sigma}_{\nu 1}\widetilde{\sigma}_{\nu 3}\widetilde{\xi}_{\ell 1}\widetilde{\xi}_{\nu 2}}{\widetilde{\mathsf{D}}_{\ell 1}\widetilde{\mathsf{D}}_{\nu 2}}} + \sqrt{\frac{\widetilde{\sigma}_e\widetilde{\sigma}_{\nu 2}}{\widetilde{\mathsf{D}}_{\ell 1}\widetilde{\mathsf{D}}_{\nu 2}}}\left(\sqrt{\widetilde{\mathcal{D}}_\ell\widetilde{\mathcal{D}}_\nu\widetilde{\xi}_{\ell 1}\widetilde{\xi}_{\nu 2}}e^{i\Phi_a} + \sqrt{\widetilde{\xi}_{\ell 2}\widetilde{\xi}_{\ell 3}\widetilde{\xi}_{\nu 1}\widetilde{\xi}_{\nu 3}}e^{i\Phi_c}\right),\\
V^{\rm th}_{e3} &= \sqrt{\frac{\widetilde{\sigma}_\mu\widetilde{\sigma}_\tau\widetilde{\sigma}_{\nu 1}\widetilde{\sigma}_{\nu 2}\widetilde{\xi}_{\ell 1}\widetilde{\xi}_{\nu 3}}{\widetilde{\mathsf{D}}_{\ell 1}\widetilde{\mathsf{D}}_{\nu 3}}} + \sqrt{\frac{\widetilde{\sigma}_e\widetilde{\sigma}_{\nu 3}}{\widetilde{\mathsf{D}}_{\ell 1}\widetilde{\mathsf{D}}_{\nu 3}}}\left(\sqrt{\widetilde{\mathcal{D}}_\ell\widetilde{\mathcal{D}}_\nu\widetilde{\xi}_{\ell 1}\widetilde{\xi}_{\nu 3}}e^{i\Phi_a} - \sqrt{\widetilde{\xi}_{\ell 2}\widetilde{\xi}_{\ell 3}\widetilde{\xi}_{\nu 1}\widetilde{\xi}_{\nu 2}}e^{i\Phi_c}\right),\\
V^{\rm th}_{\mu 1} &= -\sqrt{\frac{\widetilde{\sigma}_e\widetilde{\sigma}_\tau\widetilde{\sigma}_{\nu 2}\widetilde{\sigma}_{\nu 3}\widetilde{\xi}_{\ell 2}\widetilde{\xi}_{\nu 1}}{\widetilde{\mathsf{D}}_{\ell 2}\widetilde{\mathsf{D}}_{\nu 1}}} + \sqrt{\frac{\widetilde{\sigma}_\mu\widetilde{\sigma}_{\nu 1}}{\widetilde{\mathsf{D}}_{\ell 2}\widetilde{\mathsf{D}}_{\nu 1}}}\left(\sqrt{\widetilde{\mathcal{D}}_\ell\widetilde{\mathcal{D}}_\nu\widetilde{\xi}_{\ell 2}\widetilde{\xi}_{\nu 1}}e^{i\Phi_a} + \sqrt{\widetilde{\xi}_{\ell 1}\widetilde{\xi}_{\ell 3}\widetilde{\xi}_{\nu 2}\widetilde{\xi}_{\nu 3}}e^{i\Phi_c}\right),\\
V^{\rm th}_{\mu 2} &= \sqrt{\frac{\widetilde{\sigma}_e\widetilde{\sigma}_\tau\widetilde{\sigma}_{\nu 1}\widetilde{\sigma}_{\nu 3}\widetilde{\xi}_{\ell 2}\widetilde{\xi}_{\nu 2}}{\widetilde{\mathsf{D}}_{\ell 2}\widetilde{\mathsf{D}}_{\nu 2}}} + \sqrt{\frac{\widetilde{\sigma}_\mu\widetilde{\sigma}_{\nu 2}}{\widetilde{\mathsf{D}}_{\ell 2}\widetilde{\mathsf{D}}_{\nu 2}}}\left(\sqrt{\widetilde{\mathcal{D}}_\ell\widetilde{\mathcal{D}}_\nu\widetilde{\xi}_{\ell 2}\widetilde{\xi}_{\nu 2}}e^{i\Phi_a} + \sqrt{\widetilde{\xi}_{\ell 1}\widetilde{\xi}_{\ell 3}\widetilde{\xi}_{\nu 1}\widetilde{\xi}_{\nu 3}}e^{i\Phi_c}\right),\\
V^{\rm th}_{\mu 3} &= -\sqrt{\frac{\widetilde{\sigma}_e\widetilde{\sigma}_\tau\widetilde{\sigma}_{\nu 1}\widetilde{\sigma}_{\nu 2}\widetilde{\xi}_{\ell 2}\widetilde{\xi}_{\nu 3}}{\widetilde{\mathsf{D}}_{\ell 2}\widetilde{\mathsf{D}}_{\nu 3}}} + \sqrt{\frac{\widetilde{\sigma}_\mu\widetilde{\sigma}_{\nu 3}}{\widetilde{\mathsf{D}}_{\ell 2}\widetilde{\mathsf{D}}_{\nu 3}}}\left(\sqrt{\widetilde{\mathcal{D}}_\ell\widetilde{\mathcal{D}}_\nu\widetilde{\xi}_{\ell 2}\widetilde{\xi}_{\nu 3}}e^{i\Phi_a} - \sqrt{\widetilde{\xi}_{\ell 1}\widetilde{\xi}_{\ell 3}\widetilde{\xi}_{\nu 1}\widetilde{\xi}_{\nu 2}}e^{i\Phi_c}\right),
\end{aligned}
$$

$$\begin{aligned}
V_{\tau 1}^{\rm th} &= \sqrt{\frac{\widetilde{\sigma}_e\widetilde{\sigma}_\mu\widetilde{\sigma}_{\nu 2}\widetilde{\sigma}_{\nu 3}\widetilde{\xi}_{\ell 3}\widetilde{\xi}_{\nu 1}}{\widetilde{\mathsf{D}}_{\ell 3}\widetilde{\mathsf{D}}_{\nu 1}}} + \sqrt{\frac{\widetilde{\sigma}_\tau\widetilde{\sigma}_{\nu 1}}{\widetilde{\mathsf{D}}_{\ell 3}\widetilde{\mathsf{D}}_{\nu 1}}}\left(\sqrt{\widetilde{\mathcal{D}}_\ell\widetilde{\mathcal{D}}_\nu\widetilde{\xi}_{\ell 3}\widetilde{\xi}_{\nu 1}}e^{i\Phi_a} - \sqrt{\widetilde{\xi}_{\ell 1}\widetilde{\xi}_{\ell 2}\widetilde{\xi}_{\nu 2}\widetilde{\xi}_{\nu 3}}e^{i\Phi_c}\right), \\
V_{\tau 2}^{\rm th} &= -\sqrt{\frac{\widetilde{\sigma}_e\widetilde{\sigma}_\mu\widetilde{\sigma}_{\nu 1}\widetilde{\sigma}_{\nu 3}\widetilde{\xi}_{\ell 3}\widetilde{\xi}_{\nu 2}}{\widetilde{\mathsf{D}}_{\ell 3}\widetilde{\mathsf{D}}_{\nu 2}}} + \sqrt{\frac{\widetilde{\sigma}_\tau\widetilde{\sigma}_{\nu 2}}{\widetilde{\mathsf{D}}_{\ell 3}\widetilde{\mathsf{D}}_{\nu 2}}}\left(\sqrt{\widetilde{\mathcal{D}}_\ell\widetilde{\mathcal{D}}_\nu\widetilde{\xi}_{\ell 3}\widetilde{\xi}_{\nu 2}}e^{i\Phi_a} - \sqrt{\widetilde{\xi}_{\ell 1}\widetilde{\xi}_{\ell 2}\widetilde{\xi}_{\nu 1}\widetilde{\xi}_{\nu 3}}e^{i\Phi_c}\right), \\
V_{\tau 3}^{\rm th} &= \sqrt{\frac{\widetilde{\sigma}_e\widetilde{\sigma}_\mu\widetilde{\sigma}_{\nu 1}\widetilde{\sigma}_{\nu 2}\widetilde{\xi}_{\ell 3}\widetilde{\xi}_{\nu 3}}{\widetilde{\mathsf{D}}_{\ell 3}\widetilde{\mathsf{D}}_{\nu 3}}} + \sqrt{\frac{\widetilde{\sigma}_\tau\widetilde{\sigma}_{\nu 3}}{\widetilde{\mathsf{D}}_{\ell 3}\widetilde{\mathsf{D}}_{\nu 3}}}\left(\sqrt{\widetilde{\mathcal{D}}_\ell\widetilde{\mathcal{D}}_\nu\widetilde{\xi}_{\ell 3}\widetilde{\xi}_{\nu 3}}e^{i\Phi_a} + \sqrt{\widetilde{\xi}_{\ell 1}\widetilde{\xi}_{\ell 2}\widetilde{\xi}_{\nu 1}\widetilde{\xi}_{\nu 2}}e^{i\Phi_c}\right).
\end{aligned} \tag{69}$$

The parameter $\widetilde{\mathcal{D}}_l$, with $l = \ell, \nu$, for a normal hierarchy in the neutrino mass spectrum, must satisfy the condition:

$$\begin{aligned}
&\widetilde{m}_{11}^{f} < \widetilde{m}_{f1}, \quad \widetilde{\sigma}_{l3} > \widetilde{\mathcal{D}}_l > \widetilde{\sigma}_{l1}, \\
&\widetilde{\mathcal{D}}_l \neq +\widetilde{\sigma}_{l1} - \widetilde{\sigma}_{l2} + \widetilde{\sigma}_{l3} \quad \text{for} \quad m_{l2} \to -|m_{l2}|.
\end{aligned} \tag{70}$$

For an inverted hierarchy in the neutrino mass spectrum, the next condition must be satisfied:

$$\begin{aligned}
&\widetilde{m}_{11}^{\nu} < \widetilde{m}_{\nu 3}, \quad \widetilde{\sigma}_{\nu 1} > \widetilde{\mathcal{D}}_\nu > \widetilde{\sigma}_{\nu 3}, \\
&\widetilde{\mathcal{D}}_\nu \neq +\widetilde{\sigma}_{\nu 1} - \widetilde{\sigma}_{\nu 2} + \widetilde{\sigma}_{\nu 3}\,\text{para}\, m_{\nu 2} \to -|m_{\nu 2}|.
\end{aligned} \tag{71}$$

5.1. Numerical analysis

To evaluate how well the theoretical expressions fit the experimental data, a likelihood fit is implemented here, where the χ^2 statistic is used as the measure. The χ^2 statistic measures the difference between the observed and expected values according to the theoretical model. The method seeks the optimal values of the model parameters that minimize the error between the data and the model.

In this case, the χ^2 statistic takes the form:

$$\chi^2 = \sum_{i<j}^{3} \frac{\left(\sin^2\theta_{ij}^{\rm exp} - \sin^2\theta_{ij}^{\rm th}\right)^2}{\sigma_{\theta_{ij}}^2}. \tag{72}$$

In this expression for the χ^2 statistic, the superscript "th" is used to denote the theoretical expressions of the mixing angles of the leptons, which are obtained from the expressions:

$$\begin{aligned}
&\sin^2\theta_{12}^{\rm th} = \frac{\left|V_{e2}^{\rm th}\right|^2}{1-\left|V_{e3}^{\rm th}\right|^2}, \quad \sin^2\theta_{23}^{\rm th} = \frac{\left|V_{\mu 3}^{\rm th}\right|^2}{1-\left|V_{e3}^{\rm th}\right|^2}, \\
&\sin^2\theta_{13}^{\rm th} = \left|V_{e3}^{\rm th}\right|^2.
\end{aligned} \tag{73}$$

Meanwhile, the terms with the superscript "exp" denote the experimental data with an uncertainty $\sigma_{\theta_{ij}}$ for the mixing angles of the leptons.

For this likelihood analysis, the results from the global fit of neutrino oscillation parameters reported in Refs. [31,32] are considered. The values of the differences of the squares of the neutrino masses, $\Delta m_{ij}^2 = m_{\nu i}^2 - m_{\nu j}^2$, at BFP$\pm 1\sigma$ are

$$\begin{aligned}
\Delta m_{21}^2\left(10^{-5}\ {\rm eV}^2\right) &= 7.50_{-0.20}^{+0.22}, \\
\Delta m_{31}^2\left(10^{-3}\ {\rm eV}^2\right) &= 2.55_{-0.03}^{+0.02} \quad \text{for NH}, \\
\Delta m_{13}^2\left(10^{-3}\ {\rm eV}^2\right) &= 2.45_{-0.03}^{+0.02} \quad \text{for IH}.
\end{aligned} \tag{74}$$

The values of the differences in the mixing angles of the leptons at BFP$\pm 1\sigma$ are

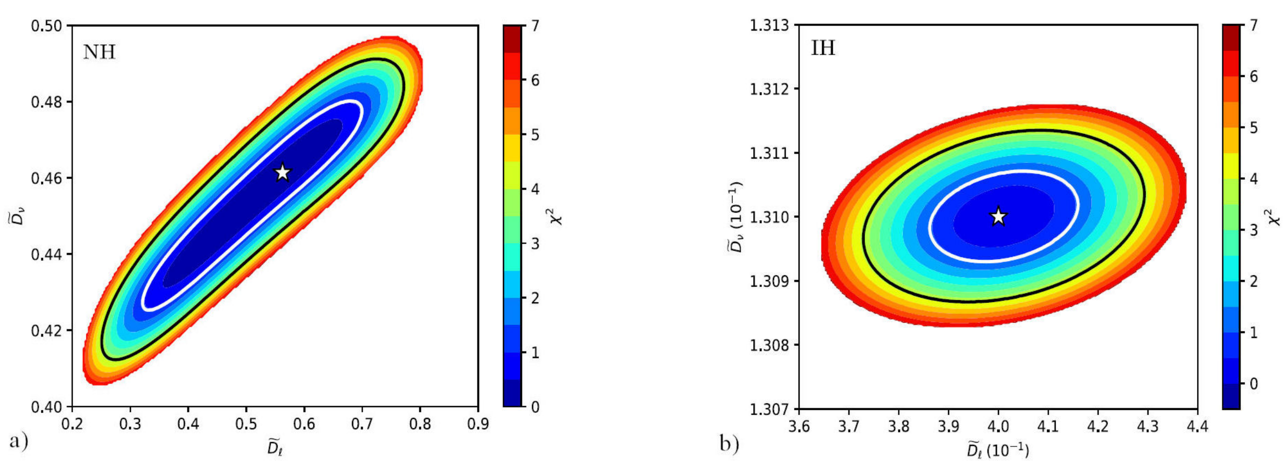

FIGURE 1. Regions of parameters for $\widetilde{D}_\ell$ and $\widetilde{D}_\nu$, where the white star represents the best fit point (BFP). The regions delimited by the white and black lines represent the allowed region at 1σ and 2σ C.L., respectively.

$$\begin{aligned}
\sin^2\theta_{12}^{\rm exp}\left(10^{-1}\right) &= 3.18 \pm 0.16,\\
\sin^2\theta_{23}^{\rm exp}\left(10^{-1}\right) &= 5.74 \pm 0.14 \text{ for NH},\\
\sin^2\theta_{23}^{\rm exp}\left(10^{-1}\right) &= 5.78^{+0.10}_{-0.17} \text{ for IH},\\
\sin^2\theta_{13}^{\rm exp}\left(10^{-2}\right) &= 2.200^{+0.069}_{-0.062} \text{ for NH},\\
\sin^2\theta_{13}^{\rm exp}\left(10^{-2}\right) &= 2.225^{+0.064}_{-0.070} \text{ for IH}.
\end{aligned} \tag{75}$$

From the definition of Δm_{ij}^2, two of the neutrino masses can be written as

$$\left.\begin{aligned}
m_{\nu 2} &= \sqrt{\Delta m_{21}^2 + m_{\nu 1}^2}\\
m_{\nu 3} &= \sqrt{\Delta m_{31}^2 + m_{\nu 1}^2}
\end{aligned}\right\} \text{ for NH,}$$
$$\left.\begin{aligned}
m_{\nu 1} &= \sqrt{\Delta m_{13}^2 + m_{\nu 3}^2}\\
m_{\nu 3} &= \sqrt{\Delta m_{21}^2 + \Delta m_{13}^2 + m_{\nu 3}^2}
\end{aligned}\right\} \text{ for IH,} \tag{76}$$

where $m_{\nu 1}$ and $m_{\nu 3}$ are the mass of the lightest neutrino for NH and IH, respectively. Furthermore, for each type of hierarchy, this neutrino mass is considered the only free parameter in the previous expressions, as the Δm_{ij}^2 are determined by the experiment.

From the expressions in Eqs. (65)-(67), (69) and (73), it is easy to conclude that for the normal [inverted] hierarchy, the χ^2 statistic depends on the parameters $\widetilde{m}_e$, $\widetilde{m}_\mu$, $\widetilde{m}_{\nu 1[3]}$, $\widetilde{m}_{\nu 2[1]}$, $\widetilde{m}_{11}^\ell$, $\widetilde{m}_{11}^\nu$, $\widetilde{D}_\ell$, $\widetilde{D}_\nu$, Φ_a, and Φ_c. However, in this likelihood analysis, the parameters $\widetilde{m}_e$, $\widetilde{m}_\mu$, and $\widetilde{m}_{\nu 2[1]}$ will not be considered as free parameters since their values are determined by experimental data.

So, the statistic parameter χ^2 depends of seven free parameters:

$$\chi^2 = \chi^2\left(\widetilde{m}_{\nu 1[3]}, \widetilde{m}_{11}^\ell, \widetilde{m}_{11}^\nu, \widetilde{D}_\ell, \widetilde{D}_\nu, \Phi_a, \Phi_c\right). \tag{77}$$

However, the χ^2 statistic depends only on three experimental values, which correspond to the leptonic flavor mixing angles. Therefore, if the seven parameters are simultaneously considered as free in the likelihood analysis, we can only determine the values of these parameters at the best-fit point (BFP). To search for the BFP through likelihood fitting, we will consider the following values for the charged lepton masses [1]

$$\begin{aligned}
m_e &= 0.51099895000 \pm 0.0000000015 \text{ MeV},\\
m_\mu &= 105.6583755 \pm 0.0000023 \text{ MeV},\\
m_\tau &= 1776.93 \pm 0.09 \text{ MeV}.
\end{aligned} \tag{78}$$

To minimize the χ^2 statistic, we perform a scan of the parameter space in which the differences of the squares of the neutrino masses and the charged lepton masses are fixed at their central values, which are given in Eqs. (75) and (78). For a normal hierarchy, we obtain the following values at the BFP for the seven free parameters and the mixing angles, with a value of the χ^2 statistic equal to 3.6184×10^{-3}:

$$\begin{aligned}
&m_{\nu 1} = 4.09 \times 10^{-3} \text{ eV}, \quad \widetilde{m}_{11}^\ell = 2.98 \times 10^{-7},\\
&\widetilde{m}_{11}^\nu = 1.15 \times 10^{-5}, \quad \widetilde{D}_\ell = 5.54871 \times 10^{-1},\\
&\widetilde{D}_\nu = 4.60288 \times 10^{-1}, \quad \Phi_a = 39^\circ, \quad \Phi_a = 300^\circ,\\
&\sin^2\theta_{12}^{\rm th} = 3.17242 \times 10^{-1}, \quad \sin^2\theta_{13}^{\rm th} = 2.20018 \times 10^{-2},\\
&\sin^2\theta_{23}^{\rm th} = 5.74517 \times 10^{-1}.
\end{aligned} \tag{79}$$

On the other hand, for an inverted hierarchy we obtain the following for a value of the χ^2 statistic equal to 6.26357×10^{-3}:

$$\begin{aligned}
&m_{\nu 3} = 2.82 \times 10^{-2} \text{ eV}, \quad \widetilde{m}_{11}^\ell = 1.02 \times 10^{-6},\\
&\widetilde{m}_{11}^\nu = 3.60 \times 10^{-1}, \quad \widetilde{D}_\ell = 4.00000 \times 10^{-1},\\
&\widetilde{D}_\nu = 1.31000 \times 10^{-1}, \quad \Phi_a = 87^\circ, \quad \Phi_a = 248.5^\circ,\\
&\sin^2\theta_{12}^{\rm th} = 3.18278 \times 10^{-1}, \quad \sin^2\theta_{13}^{\rm th} = 2.22517 \times 10^{-2},\\
&\sin^2\theta_{23}^{\rm th} = 5.79041 \times 10^{-1}.
\end{aligned} \tag{80}$$

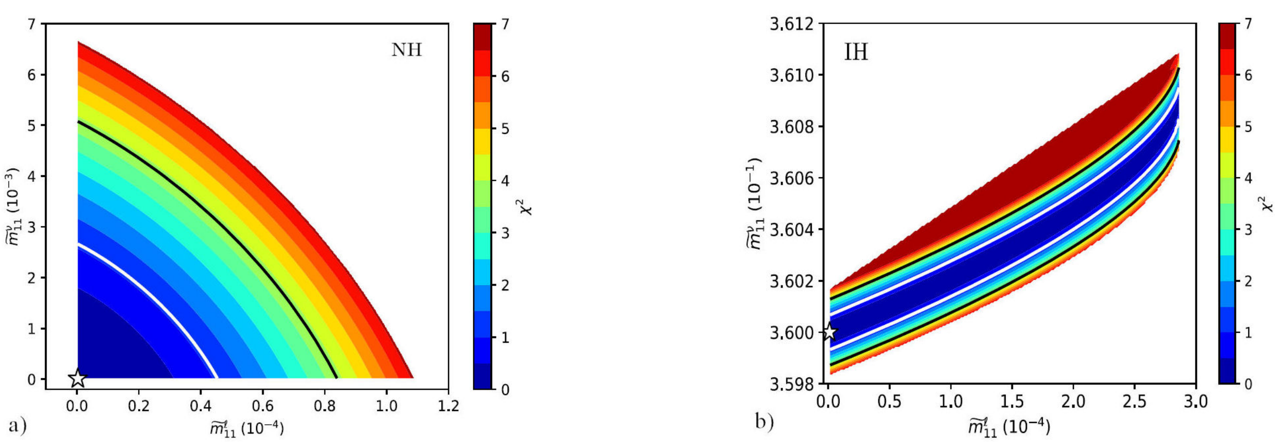

FIGURE 2. Parameter regions for $\widetilde{m}_{11}^\ell$ and $\widetilde{m}_{11}^\nu$, where the white star represents the BFP. The regions bounded by the white and black lines represent the allowed region at 1σ and 2σ C.L., respectively.

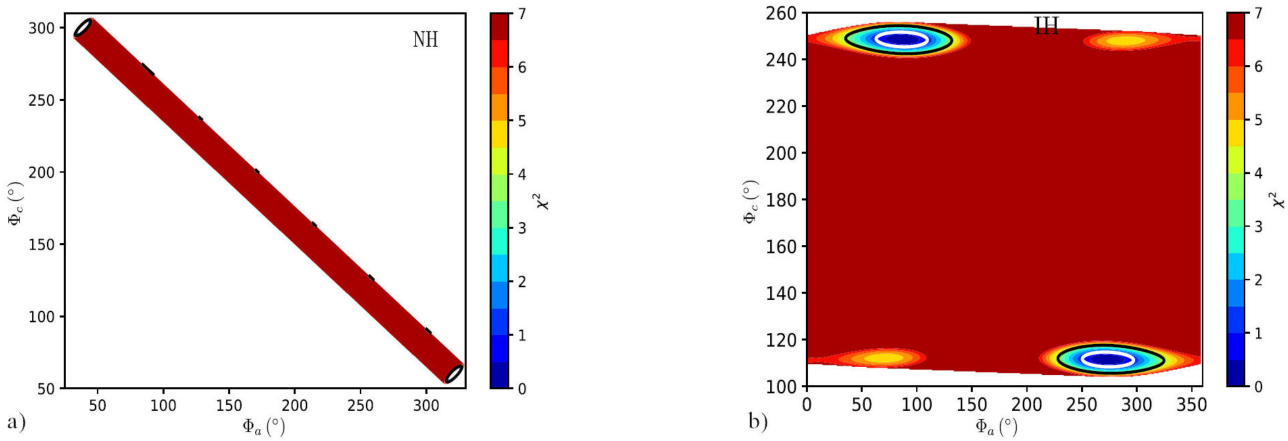

FIGURE 3. Parameter regions for Φ_a and Φ_c.

Now, since we already know the numerical values of the seven free parameters at the BFP, the next step is to perform new likelihood fits in which the values of five or six free parameters are fixed so that the χ^2 statistic has one or two degrees of freedom.

In order to determine the allowed regions of the free parameters, the values of Δm_{ij}^2 and the charged lepton masses are fixed at the BFP values given in Eqs. (74) and (78). Meanwhile, $\widetilde{m}_{\nu 1[3]}$, $\widetilde{m}_{11}^{\ell}$, $\widetilde{m}_{11}^{\nu}$, $\widetilde{D}_{\ell}$, $\widetilde{D}_{\nu}$, Φ_a, and Φ_c are fixed at the values given in Eqs. (79) and (80).

Thus, in the case where the statistic is $\chi^2 = \chi^2\left(\widetilde{D}_{\ell}, \widetilde{D}_{\nu}\right)$, this implies one degree of freedom, yielding the following results at 1σ C.L.

$$\widetilde{D}_{\ell} = \begin{cases} \left(5.549^{+1.428}_{-2.339}\right) \times 10^{-1} \text{ for NH,} \\ \left(4.00^{+0.16}_{-0.14}\right) \times 10^{-1} \text{ for IH,} \end{cases}$$
$$\widetilde{D}_{\nu} = \begin{cases} \left(4.603^{+0.196}_{-0.349}\right) \times 10^{-1} \text{ for NH,} \\ \left(1.3100^{+0.0008}_{-0.0007}\right) \times 10^{-1} \text{ for IH.} \end{cases} \tag{81}$$

For the normal and inverted hierarchies, we obtain $\chi^2 = 5.41 \times 10^{-3}$ and $\chi^2 = 3.59 \times 10^{-4}$ respectively. In Fig. 1, we show the parameter regions for $\widetilde{D}_{\ell}$ and $\widetilde{D}_{\nu}$, where the white star represents the BFP. The regions bounded by the white and black lines represent the allowed region at 1σ and 2σ C.L., respectively. The left panel corresponds to the normal hierarchy, with both parameters of order 10^{-1}. The right panel corresponds to the inverted hierarchy, where both parameters are also of order 10^{-1}.

In the case where the statistic is $\chi^2 = \chi^2\left(\widetilde{m}_{11}^{\ell}, \widetilde{m}_{11}^{\nu}\right)$, this implies one degree of freedom, yielding the following results at 1σ C.L.

$$\widetilde{m}_{11}^{\ell} = \begin{cases} \left(2.98^{+451.65}_{-2.88}\right) \times 10^{-7} \text{ for NH,} \\ \left(1.02^{+286.55}_{-1.00}\right) \times 10^{-6} \text{ for IH,} \end{cases}$$
$$\widetilde{m}_{11}^{\nu} = \begin{cases} \left(1.15^{+265.81}_{-1.14}\right) \times 10^{-5} \text{ for NH,} \\ \left(3.600^{+0.010}_{-0.007}\right) \times 10^{-1} \text{ for IH.} \end{cases} \tag{82}$$

For the normal and inverted hierarchies, we obtain $\chi^2 = 3.20 \times 10^{-3}$ and $\chi^2 = 5.98 \times 10^{-3}$, respectively. In Fig. 2, we show the parameter regions for $\widetilde{m}_{11}^{\ell}$ and $\widetilde{m}_{11}^{\nu}$, where the white star represents the BFP. The regions bounded by the white and black lines represent the allowed region at 1σ and 2σ C.L., respectively. The left panel corresponds to the normal hierarchy, where the parameter $\widetilde{m}_{11}^{\ell}$ is of order 10^{-4} and the parameter $\widetilde{m}_{11}^{\nu}$ is of order 10^{-3}. The right panel corresponds to the inverted hierarchy, where the parameter $\widetilde{m}_{11}^{\ell}$ is of order 10^{-4} and the parameter $\widetilde{m}_{11}^{\nu}$ is of order 10^{-1}.

In the case where the statistic is $\chi^2 = \chi^2\left(\Phi_a, \Phi_c\right)$, this implies one degree of freedom, yielding the following results at 1σ C.L.

$$\Phi_a = \begin{cases} \left(39^{+4.0}_{-3.0}\right)^{\circ} \text{ for NH,} \\ \left(87^{+28}_{-17}\right)^{\circ} \text{ for IH,} \end{cases}$$
$$\Phi_c = \begin{cases} \left(300^{+2.0}_{-3.0}\right)^{\circ} \text{ for NH,} \\ (248.5 \pm 3.0)^{\circ} \text{ for IH.} \end{cases} \tag{83}$$

For the normal and inverted hierarchies, we obtain $\chi^2 = 2.58 \times 10^{-3}$ and $\chi^2 = 6.33 \times 10^{-3}$, respectively. In Fig. 3, we show the complete parameter regions for the phase factors Φ_a and Φ_c. In Fig. 4, we show a zoom-in of the parameter regions for Φ_a and Φ_c, where the white star represents the BFP. The regions bounded by the white and black lines represent the allowed region at 1σ and 2σ C.L., respectively. The left panel corresponds to the normal hierarchy. The right panel corresponds to the inverted hierarchy.

In the case where the statistic is $\chi^2 = \chi^2\left(m_{\nu 1[3]}\right)$, this implies two degrees of freedom, yielding the following results at 1σ C.L.

$$\begin{aligned} m_{\nu 1} &= \left(4.09^{+0.13}_{-0.12}\right) \times 10^{-3} \text{ eV for NH,} \\ m_{\nu 3} &= (2.82 \pm 0.01) \times 10^{-2} \text{ eV for IH.} \end{aligned} \tag{84}$$

For the normal and inverted hierarchies, we obtain $\chi^2 = 3.39 \times 10^{-3}$ and $\chi^2 = 6.15 \times 10^{-3}$, respectively.

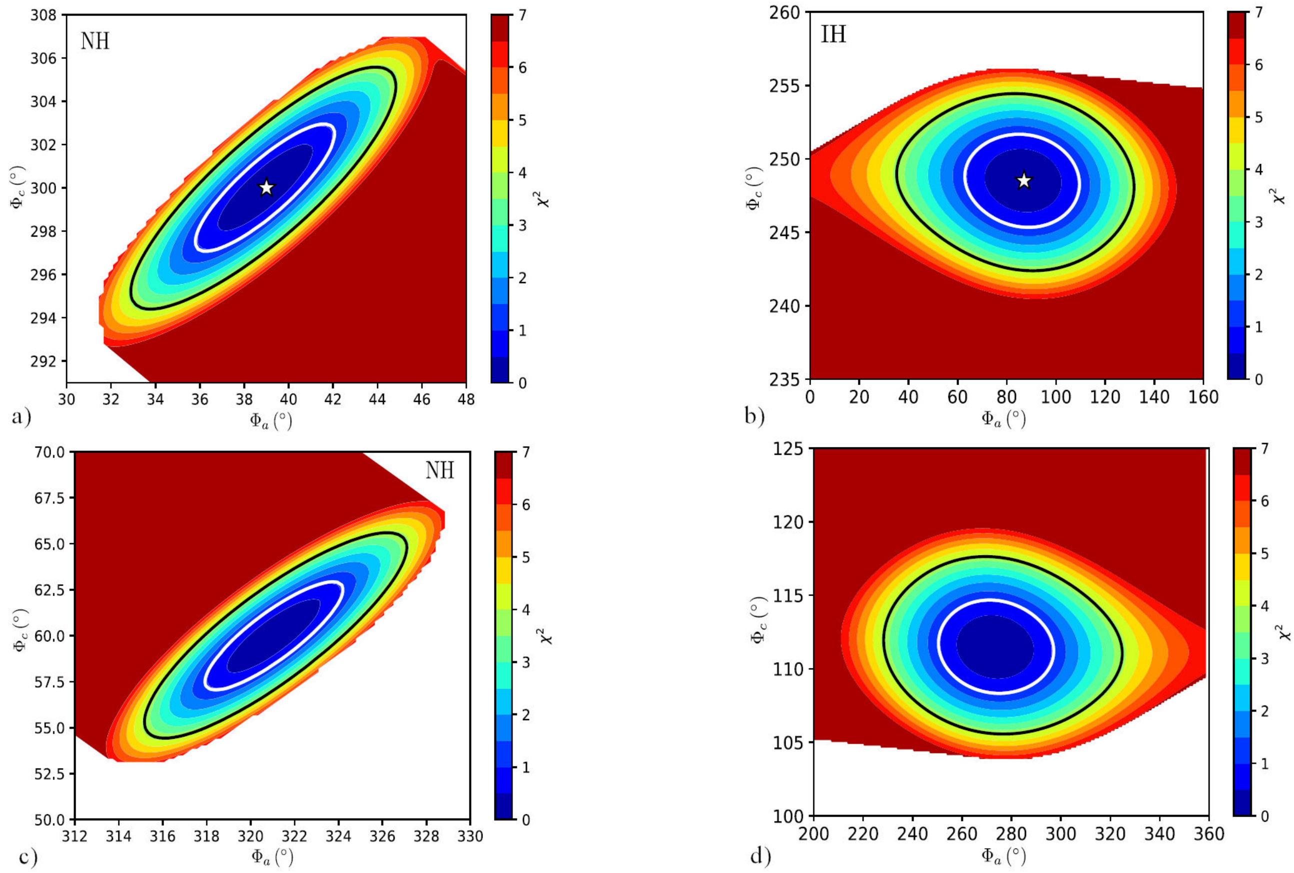

FIGURE 4. Amplification of the parameter regions for Φ_a and Φ_c, where the white star represents the BFP. The regions bounded by the white and black lines represent the allowed region at 1σ and 2σ C.L., respectively.

From the results obtained in the previous likelihood fits, for a normal hierarchy, the leptonic mixing angles have the following average values at 1σ C.L.

$$\begin{aligned}
\sin^2\theta_{12}^{\rm th} &= \left(3.172^{+0.051}_{-0.057}\right)\times 10^{-1},\\
\sin^2\theta_{13}^{\rm th} &= \left(2.199^{+0.046}_{-0.066}\right)\times 10^{-2},\\
\sin^2\theta_{23}^{\rm th} &= \left(5.744^{+0.054}_{-0.097}\right)\times 10^{-1},
\end{aligned} \tag{85}$$

whereas for an inverted hierarchy at 1σ C.L.

$$\begin{aligned}
\sin^2\theta_{12}^{\rm th} &= \left(3.183^{+0.054}_{-0.060}\right)\times 10^{-1},\\
\sin^2\theta_{13}^{\rm th} &= \left(2.225\pm 0.069\right)\times 10^{-2},\\
\sin^2\theta_{23}^{\rm th} &= \left(5.787^{+0.073}_{-0.059}\right)\times 10^{-1}.
\end{aligned} \tag{86}$$

With these values for the flavor mixing angles, it can be seen that the current experimental values for neutrino oscillations are correctly reproduced.

6. Conclusions

A systematic and detailed model-independent analysis of fermionic flavor masses and mixings was developed. First, we have demonstrated that fermion mass matrices can be consistently cast into a canonical weak–basis form with vanishing $(1,3)$ and $(3,1)$ entries, motivated by the hierarchical structure of fermion masses and mixings and without invoking dynamical texture assumptions. This formulation naturally encompasses both Hermitian and complex symmetric cases, providing a unified description of Dirac and Majorana fermion mass terms. Then, it is required that the rotated matrix satisfies the internal symmetry of being either Hermitian or complex symmetric, in order to express it in polar form and factor out the phases. Both the real symmetric matrix and the PMNS flavor mixing matrix are expressed in terms of the fermion masses and some free parameters.

To evaluate how well the theoretical expressions for the leptonic flavor mixing angles reproduce experimental data, a likelihood test using the χ^2 statistic was implemented. The results of the χ^2 fit show that the theoretical expressions obtained for the PMNS flavor mixing matrix correctly reproduce the current experimental data on neutrino oscillations. The difference between representing the lepton mass matrix as Hermitian or as complex symmetric lies solely in the form of the diagonal matrix of phase factors.

1. S. Navas *et al*., Review of particle physics, *Phys. Rev. D* **110** (2024) 030001, https://doi.org/10.1103/PhysRevD.110.030001
2. B. Garbrecht, Why is there more matter than antimatter? Calculational methods for leptogenesis and electroweak baryogenesis, *Prog. Part. Nucl. Phys.* **110** (2020) 103727, https://doi.org/10.1016/j.ppnp.2019.103727
3. S.Weinberg, Models of lepton and quark masses, *Phys. Rev. D* **101** (2020) 035020, https://doi.org/10.1103/PhysRevD.101.035020
4. A. Abokhalil, The Higgs Mechanism and Higgs Boson: Unveiling the Symmetry of the Universe (2023), https://doi.org/10.48550/arXiv.2306.01019
5. P. Langacker, The Standard Model and Beyond, Series in high energy physics, cosmology, and gravitation (CRC Press, Taylor & Francis Group, 2017), URL https://books.google.com.mx/books?id=QHRfAQAACAAJ.
6. Y. Fukuda *et al*., Measurements of the solar neutrino flux from Super-Kamiokande's first 300 days, *Phys. Rev. Lett*. **81** (1998) 1158, https://doi.org/10.1103/PhysRevLett.81.1158
7. Q. R. Ahmad *et al.*, Direct evidence for neutrino flavor transformation from neutral current interactions in the Sudbury Neutrino Observatory, *Phys. Rev. Lett*. **89** (2002) 011301, https://doi.org/10.1103/PhysRevLett.89.011301
8. P. Minkowski, $\mu \to e\gamma$ at a Rate of One Out of 109 Muon Decays?, *Phys. Lett. B* **67** (1977) 421, https://doi.org/10.1016/0370-2693(77)90435-X
9. M. Aker *et al.*, Improved Upper Limit on the Neutrino Mass from a Direct Kinematic Method by KATRIN, *Phys. Rev. Lett.* **123** (2019) 221802, https://doi.org/10.1103/PhysRevLett.123.221802
10. E. Barradas-Guevara *et al.*, Lepton CP violation in a v2HDM with flavor, *Phys. Rev. D* **97** (2018) 035003, https://doi.org/10.1103/PhysRevD.97.035003
11. C. Jarlskog, A Basis Independent Formulation of the Connection Between Quark Mass Matrices, CP Violation and Experiment, *Z. Phys. C* **29** (1985) 491, https://doi.org/10.1007/BF01565198
12. J. Schechter and J. W. F. Valle, Neutrino Masses in SU(2) x U(1) Theories, *Phys. Rev. D* **22** (1980) 2227, https://doi.org/10.1103/PhysRevD.22.2227
13. H. Fritzsch, Calculating the Cabibbo Angle, *Phys. Lett. B* **70** (1977) 436, https://doi.org/10.1016/0370-2693(77)90408-7
14. H. Fritzsch, Quark Masses and Flavor Mixing, *Nucl. Phys. B* **155** (1979) 189, https://doi.org/10.1016/0550-3213(79)90362-6
15. R. Gatto, G. Sartori, and M. Tonin, Weak Selfmasses, Cabibbo Angle, and Broken SU(2) x SU(2), *Phys. Lett. B* **28** (1968) 128, https://doi.org/10.1016/0370-2693(68)90150-0
16. H. Fritzsch and Z.-z. Xing, Mass and flavor mixing schemes of quarks and leptons, *Prog. Part. Nucl. Phys.* **45** (2000) 1, https://doi.org/10.1016/S0146-6410(00)00102-2
17. G. C. Branco, L. Lavoura, and J. P. Silva, CP Violation, **103** (1999), https://doi.org/10.1093/oso/9780198503996.001.0001
18. C. D. Froggatt and H. B. Nielsen, Hierarchy of Quark Masses, Cabibbo Angles and CP Violation, *Nucl. Phys. B* **147** (1979) 277, https://doi.org/10.1016/0550-3213(79)90316-X
19. M. Leurer, Y. Nir, and N. Seiberg, Mass matrix models, *Nucl. Phys. B* **398** (1993) 319, https://doi.org/10.1016/0550-3213(93)90112-3
20. P. Ramond, R. G. Roberts, and G. G. Ross, Stitching the Yukawa quilt, *Nucl. Phys. B* **406** (1993) 19, https://doi.org/10.1016/0550-3213(93)90159-M
21. G. C. Branco, D. Emmanuel-Costa, and R. Gonzalez Felipe, Texture zeros and weak basis transformations, *Phys. Lett. B* **477** (2000) 147, https://doi.org/10.1016/S0370-2693(00)00193-3
22. J. Bernabeu, G. C. Branco, and M. Gronau, CP Restrictions on Quark Mass Matrices, *Phys. Lett. B* **169** (1986) 243, https://doi.org/10.1016/0370-2693(86)90659-3
23. G. C. Branco, M. N. Rebelo, and J. I. Silva-Marcos, Large neutrino mixing with universal strength of Yukawa couplings, *Phys. Rev. D* **62** (2000) 073004, https://doi.org/10.1103/PhysRevD.62.073004
24. K. Harayama and N. Okamura, Exact parametrization of the mass matrices and the KM matrix, *Phys. Lett. B* **387** (1996) 614, https://doi.org/10.1016/0370-2693(96)01079-9
25. E. Barradas-Guevara, O. Félix-Beltrán, and E. Rodríguez-Jáuregui, Trilinear self-couplings in an S(3) flavored Higgs model, *Phys. Rev. D* **90** (2014) 095001, https://doi.org/10.1103/PhysRevD.90.095001
26. F. González Canales, A. Mondragón, and M. Mondragón, The S3 flavour symmetry: Neutrino masses and mixings, *Fortschritte der Physik* **61** (2013) 546, https://doi.org/10.1002/prop.201200121
27. F. González Canales *et al.*, Quark sector of S3 models: classification and comparison with experimental data, *Phys. Rev. D* **88** (2013) 096004, https://doi.org/10.1103/PhysRevD.88.096004
28. R. Acciarri *et al*., Long-Baseline Neutrino Facility (LBNF) and Deep Underground Neutrino Experiment (DUNE): Conceptual Design Report, Volume 1: The LBNF and DUNE Projects (2016), https://doi.org/10.48550/arXiv.1601.05471
29. E. Barradas-Guevara, O. Félix-Beltrán, and F. Gonzalez-Canales, Deviation to the Tri-Bi-Maximal flavor pattern and equivalent classes, *Int. J. Mod. Phys. A* **38** (2023) 2350031, https://doi.org/10.1142/S0217751X23500318
30. O. Félix-Beltrán *et al.*, Analysis of the quark sector in the 2HDM with a four-zero Yukawa texture using the most recent data on the CKM matrix, *Phys. Lett. B* **742** (2015) 347, https://doi.org/10.1016/j.physletb.2015.02.003
31. P. F. De Salas *et al.*, Chi2 profiles from Valencia neutrino global fit,https://doi.org/10.5281/zenodo.4726908.

32. P. F. de Salas *et al.*, 2020 global reassessment of the neutrino oscillation picture, *JHEP* **02** (2021) 071, https://doi.org/10.1007/JHEP02(2021)071
33. M. Bauer and T. Plehn, Yet Another Introduction to Dark Matter: The Particle Physics Approach, vol. 959 of Lecture Notes in Physics (Springer, 2019), https://doi.org/10.1007/978-3-030-16234-4
34. C. Rigouzzo and S. Zell, Coupling metric-affine gravity to the standard model and dark matter fermions, *Phys. Rev. D* **108** (2023) 124067, https://doi.org/10.1103/PhysRevD.108.124067
35. W. J. Wolf and P. G. Ferreira, Underdetermination of dark energy, *Phys. Rev. D* **108** (2023) 103519, https://doi.org/10.1103/PhysRevD.108.103519
36. V. S. Mummidi, P. Lamba, and S. K. Vempati, Supersymmetry: a decade after Higgs discovery, *Indian J. Phys*. **97** (2023) 3315, https://doi.org/10.1007/s12648-023-02812-x
37. S. Antusch *et al.*, Singling out SO(10) GUT models using recent PTA results, *Phys. Rev. D* **108** (2023) 095053, https://doi.org/10.1103/PhysRevD.108.095053
38. N. Aghanim *et al*., Planck 2018 results. VI. Cosmological parameters, *Astron. Astrophys.* **641** (2020) A6, https://doi.org/10.1051/0004-6361/201833910